

# CONSTRAINT-SATISFYING KRYLOV SOLVERS FOR STRUCTURE-PRESERVING DISCRETISATIONS

JAMES JACKAMAN AND SCOTT MACLACHLAN

**ABSTRACT.** A key consideration in the development of numerical schemes for time-dependent partial differential equations (PDEs) is the ability to preserve certain properties of the continuum solution, such as associated conservation laws or other geometric structures of the solution. There is a long history of the development and analysis of such *structure-preserving* discretisation schemes, including both proofs that standard schemes have structure-preserving properties and proposals for novel schemes that achieve both high-order accuracy and exact preservation of certain properties of the continuum differential equation. When coupled with implicit time-stepping methods, a major downside to these schemes is that their structure-preserving properties generally rely on *exact* solution of the (possibly nonlinear) systems of equations defining each time-step in the discrete scheme. For small systems, this is often possible (up to the accuracy of floating-point arithmetic), but it becomes impractical for the large linear systems that arise when considering typical discretisations of space-time PDEs. In this paper, we propose a modification to the standard flexible generalised minimum residual (FGMRES) iteration that enforces selected constraints on approximate numerical solutions. We demonstrate its application to both systems of conservation laws and dissipative systems.

## 1. INTRODUCTION

Since the invention of modern digital computers, there has been intense study of numerical methods for the approximation of solutions to systems of partial differential equations (see, for example, [23]). Within this study has arisen a specialisation of methods for continuum PDEs that have associated geometric properties, such as Hamiltonian and reversible systems, problems posed over Lie groups, or systems with other structures deemed noteworthy. This field is quite mature, with numerous research papers and textbooks published in the area known as *geometric numerical integration* [8, 21, 29, 40], but also with a continuing interest in the development and analysis of new methods within the class continuing to the present (cf., for example, [9, 24, 41]). The present work is motivated by the impracticality of an underlying assumption in this work, that the linear and nonlinear systems of equations associated with these discretisations can be effectively solved to high-enough accuracy to guarantee preservation of geometric structure (at least up to machine precision of floating-point arithmetic).

The solution of systems of equations is generally required by any implicit numerical scheme for time-dependent PDEs. While some geometric schemes can utilise explicit integrators (e.g., [43]), schemes typically rely on implicit discretisation to achieve both stability and their geometric properties. When considering numerical solution of small systems of ordinary differential equations, we rarely account for the true computational burden of solving linear and nonlinear systems exactly, namely using LU factorisation to solve the linear systems, and Newton's method to high tolerance for nonlinear systems. For systems of ODEs that arise from the method-of-lines (or other) discretisation of space-time PDEs, however, these assumptions are often impractical, due simply to the computational cost of exact solutions of linear systems, or of solving either linear or nonlinear systems to high tolerances.

Because of this essential issue, some attention has been drawn to the development of Krylov methods for the solution of systems with Hamiltonian or symplectic structure [4, 5, 46]. The inherent idea in this work (and its generalisations [6, 30]) is to build the Krylov space so that all vectors in the Krylov space satisfy the expected properties of the solution. In the Hamiltonian case, we consider a symmetric matrix,  $H$ , of dimension  $2m \times 2m$ , and skew-symmetric matrix,  $J = \begin{bmatrix} 0 & I \\ -I & 0 \end{bmatrix}$ , where the blocks of  $J$  are of size  $m \times m$ , and

---

*Date:* June 21, 2023.

This work was partially supported by an NSERC Discovery Grant (SM and JJ) and the ERCIM Alain Bensoussan Fellowship Programme (JJ).

the symplectic Lanczos algorithm [6] generates a  $J$ -orthogonal basis for the Krylov spaces of even dimension. In [30], it is shown that this can be used to generate energy-preserving approximate numerical solutions of the ODE system  $\frac{dy}{dt} = JHy$ . To our knowledge, these approaches have not been extended beyond variations on Hamiltonian/symplectic structure, or to broader classes of conservation laws. In this paper, we propose an alternate approach that is more costly, but also more flexible, allowing us to work with arbitrary conservation laws, regardless of their origin or geometric structure.

The essential ingredients of our approach are as follows. We consider classes of space-time PDEs that have associated geometric properties, either in terms of related conserved quantities or dissipation laws. For any given problem, we rely upon a structure-preserving discretisation; for our problems, this will take the form of a spatial semi-discretisation that preserves the continuum properties (see, for example, [14, 24, 26]) coupled with an implicit-in-time Runge-Kutta (RK) method that preserves these properties now in the discrete setting (at each timestep) (cf. [41]). At the discrete level, this gives us a nonlinear or linear system to be solved at each timestep (we consider only the linear case herein), defining the approximate solution at the next timestep in terms of that at the current timestep, along with a list of constraint functionals (e.g., linear or bilinear forms, although more general constraints are possible) that have prescribed values for the approximate solution at the next time step. In this paper, we describe a modification to the standard flexible GMRES (FGMRES) algorithm [38, 39] that provides an approximate solution to the linear system that simultaneously satisfies (or attempts to satisfy) the constraints associated with the list of functionals given.

While two variants are described, the main approach here can be implemented in a relatively non-intrusive way to an existing FGMRES implementation, requiring only access to the basis for the (preconditioned) Krylov space once the FGMRES convergence criterion is (close to) satisfied. Notably, the method can be implemented without restrictions on the use of any (sensible) preconditioning strategy. Furthermore, the approach is viable for any Krylov method that maintains (i.e., stores) a basis for the Krylov space, although it is particularly well-suited to the structure of calculation within GMRES and FGMRES. The main expense in the method is the solution of a constrained minimisation problem, for which we make use of a sequential quadratic programming approach [28] as implemented in SciPy [45]. We note that both our intent and approach is quite different from that in [7, 33], which focus on local and global conservation (of mass) for hyperbolic conservation laws by *unmodified* iterative methods for solution of the resulting linear and nonlinear systems. We also note the similarity between our approach and that used in [17], where solutions to a given linear system and its shifted counterpart are computed from the same Krylov space by retaining similar information with additional computation.

The remainder of this paper is organised as follows. In Section 2, we give an overview of structure-preserving discretisation based on the finite-element plus implicit RK methodology. Then, in Section 3, we present the main contribution here, of the modified constraint-satisfying form of the FGMRES algorithm, and some discussion of its limitations and possible extensions. Numerical examples are presented in Section 4, followed by concluding remarks in Section 5.

## 2. STRUCTURE-PRESERVING DISCRETISATION

Many PDEs (or systems of PDEs) possess some underlying structure, be it symplectic, variational, symmetry preserving or conserved quantities, and much work has gone into developing discretisation frameworks that preserve such structures [8, 21, 34, 35]. Here we focus on the case of linear (systems of) PDEs, where the structure-preserving properties of such discretisation depends on suitable solution of the underlying linear systems in an implicit time discretisation strategy. We note that the ideas outlined here may be generalised to nonlinear systems of PDEs and nonlinear solvers, as discussed in Remark 3.4.

For simplicity, we focus on numerical schemes that possess associated conservation laws, but note that the methodology can be applied to any underlying structure that can be expressed in a similar framework (including the case of a dissipative system discussed in Section 2.3). We consider discretisation using the method-of-lines approach, coupling well-chosen spatial finite-element methods with implicit RK temporal integrators. The specific choice of the spatial finite-element method depends strongly on the problem at hand; it is rare that standard choices of continuous piecewise polynomial (Lagrange) spaces yield Galerkin discretisations with significant conservative properties, although summation-by-parts methods provide an alternative that does just this, cf. [18, 19]. In general, we consider a continuum PDE or system of PDEs,

$u_t + Lu = g$ , posed on the time interval  $[0, T]$  and spatial domain,  $\Omega$ , with suitable boundary conditions on  $\partial\Omega$ . We pass from the PDE form to a variational formulation by multiplying by a (scalar or vector) test function,  $\phi$ , and (typically) integrating by parts on some or all of the terms in  $\langle Lu, \phi \rangle$ . Then, we choose suitable discrete subspace(s) for  $u$  and  $\phi$ , leading to the semi-discretised form of the PDE, which we write as  $\mathbf{z}_t = \mathbf{h}(t, \mathbf{z})$  for  $\mathbf{z}(t) \in \mathbb{R}^d$  and  $t \in [0, T]$ . Details of this process are described for three model problems in the following subsections. We note that there is a one-to-one correspondence between the discrete values of  $\mathbf{z}(t)$  at time  $t$  and a function on  $\Omega$  that is the finite-element approximation to  $u(t, x)$  for  $x \in \Omega$ . We also assume that this semi-discretisation process preserves some number of continuum conservation laws that, after discretisation, can be expressed as  $\frac{d}{dt} g_\ell(\mathbf{z}(t)) = 0$ .

For the temporal discretisation, we consider the symplectic Gauss-Legendre family of implicit RK methods (GLRK). For a problem of the form  $\mathbf{z}_t = \mathbf{h}(t, \mathbf{z})$ , we write the  $s$ -stage symplectic RK method as

$$\mathbf{z}^{n+1} = \mathbf{z}^n + \tau_n \sum_{i=1}^s b_i \mathbf{k}^i \text{ with } \mathbf{k}^i = \mathbf{h} \left( t^n + c_i \tau_n, \mathbf{z}^n + \tau_n \sum_{j=1}^s a_{ij} \mathbf{k}^j \right),$$

where  $\mathbf{z}^n$  is the approximation to  $\mathbf{z}(t_n)$  for  $t_n \in [0, T]$ ,  $\tau_n = t_{n+1} - t_n$ , and the values  $\{a_{ij}\}$ ,  $\{b_i\}$ , and  $\{c_i\}$  come from the *Butcher Tableau* for the RK scheme. The vectors  $\mathbf{k}^i$  denote an approximation to the derivative of  $\mathbf{z}(t)$  at the stage times  $t^n + c_i \tau_n$ . Here, we take  $\{c_i\}$  to be the zeroes of the shifted Legendre polynomial  $\frac{d^s}{dx^s} (x^s(x-1)^s)$ , and the other coefficients of (2) are described by

$$a_{ij} = \int_0^{c_i} \mathcal{L}_j(\tau) d\tau, \quad b_i = \int_0^1 \mathcal{L}_i(\tau) d\tau,$$

where  $\mathcal{L}_i$  is the  $i$ -th Lagrange polynomial. We note that, as proven in [21, IV.2.1], this family of methods preserves all quadratic invariants, meaning that  $g_\ell(\mathbf{z}^{n+1}) = g_\ell(\mathbf{z}^n)$  if  $g_\ell(\mathbf{z})$  is a polynomial in  $\mathbf{z}$  of degree at most two. For simplicity, we typically employ the lowest-order method in this family, the implicit midpoint method. We note that this, in turn, is equivalent to the popular Crank-Nicolson temporal discretisation methodology, under the assumption that  $\mathbf{h}(t, \mathbf{z})$  is a linear operator.

Practically, (2) results in a coupled system of equations to solve for  $\{\mathbf{k}^i\}$  at each time step. While, in general, this system is nonlinear (due to dependence on the nonlinear function  $\mathbf{h}(t, \mathbf{z})$ ), we consider the case of linear PDEs, leading to linear systems of equations of dimension  $\mathbb{R}^{sd}$ , with one vector  $\mathbf{k}^i \in \mathbb{R}^d$  for each stage in the RK scheme. Using standard notation, we write this linear system as  $\mathcal{A}\mathbf{x} = \mathbf{f}$ , suppressing dependence on the time step and noting that matrix  $\mathcal{A} \in \mathbb{R}^{sd \times sd}$  is not the same as the coefficients  $\{a_{ij}\}$  in the Butcher Tableau. We note that in the special case of the Crank-Nicolson discretisation, this linear system can also be solved directly for  $\mathbf{z}^{n+1}$  instead of the single stage value  $\mathbf{k}^1$ , which we do in that case.

**2.1. The Linear Korteweg-De Vries Equation.** The linear Korteweg-De Vries (KdV) equation is given by

$$u_t + u_x + u_{xxx} = 0,$$

where we consider  $t \in [0, T]$  and  $x \in \Omega = [0, X]$ , with  $u(t, x)$  being periodic with period  $X$ , and initial condition  $u(0, x) = u_0(x)$ . Just as in the case of the nonlinear KdV equation, this system has several nontrivial invariants. For the sake of exposition, we focus on three of these, namely mass conservation,  $\frac{d}{dt} \int_\Omega u dx = 0$ , momentum conservation,  $\frac{d}{dt} \int_\Omega \frac{1}{2} u^2 dx = 0$ , and energy conservation,  $\frac{d}{dt} \int_\Omega \frac{1}{2} u_x^2 - \frac{1}{2} u^2 dx = 0$ .

Given the dependence on a high-order spatial derivative in (2.1), the spatial discretisation requires either higher-order finite-element methods with enhanced continuity or rewriting the equations to allow use of standard Lagrange basis functions. We choose the latter, rewriting the linear KdV equation as the equivalent system

$$u_t + v_x = 0, \quad v - u - w_x = 0, \quad w - u_x = 0.$$

Partitioning the interval,  $\Omega$ , as  $0 = x_0 < \dots < x_m < \dots < x_{M_x} = X$  with an arbitrary element  $\mathcal{J}_m := (x_m, x_{m+1})$ , we define the spatial finite-element space as follows.

**Definition 2.1** (One dimensional finite-element spaces). Let  $\mathbb{P}_q(\mathcal{J}_m)$  denote the space of polynomials of degree no more than  $q$  on the element  $\mathcal{J}_m$ . Then, the discontinuous finite-element space  $\mathbb{V}_q$  is given by

$$\mathbb{V}_q = \{U : \Omega \rightarrow \mathbb{R} : U|_{\mathcal{J}_m} \in \mathbb{P}_q(\mathcal{J}_m) \text{ for } m = 0, \dots, M_x - 1\}.$$

Note that the dimension of  $\mathbb{V}_q$  is given by  $(q+1)M_x$

Before introducing the finite element method, we must first define the weak first spatial derivative for the discontinuous function space.

**Definition 2.2** (Spatial derivative operator). Let  $U \in \mathbb{V}_q$ , then we define  $\mathcal{G}_h : \mathbb{V}_q \rightarrow \mathbb{V}_q$  such that

$$\int_{\Omega} \mathcal{G}_h(U) \phi = \sum_{m=0}^{M_x-1} \int_{\mathcal{J}_m} U_x \phi - \llbracket U_m \rrbracket \{\phi_m\} \quad \forall \phi \in \mathbb{V}_q,$$

where

$$\llbracket U_m \rrbracket = \lim_{y \nearrow x_m} U(x) - \lim_{y \searrow x_m} U(x)$$

is the jump in  $U(x)$  at  $x = x_m$  and

$$\{\phi_m\} = \frac{1}{2} \left( \lim_{y \nearrow x_m} \phi(x) + \lim_{y \searrow x_m} \phi(x) \right)$$

the average of the two one-sided limits at  $x_m$ .

With this definition in mind, our conservative spatial finite-element discretisation of (2.1) is given by seeking  $U, V, W \in \mathbb{V}_q$  such that

$$\begin{aligned} \int_{\Omega} (U_t + \mathcal{G}_h(V)) \phi \, dx &= 0 & \forall \phi \in \mathbb{V}_q \\ \int_{\Omega} (V - U - \mathcal{G}_h(W)) \psi \, dx &= 0 & \forall \psi \in \mathbb{V}_q \\ \int_{\Omega} (W - \mathcal{G}_h(U)) \chi \, dx &= 0 & \forall \chi \in \mathbb{V}_q, \end{aligned}$$

subject to initialising  $U$ ,  $V$ , and  $W$  based on some initial data  $U(0, x)$ . We note there are similarities between the first-order system form of the linear KdV equation and the design of local discontinuous Galerkin methods; see, for example, [25, 47]; however, we use only the central fluxes defined above (see [26, §4]). We also note that, in contrast to the earlier discussion, (2.1) takes the form of a differential-algebraic equation (DAE), for which Runge-Kutta methods remain well-defined [22].

We fully discretise the system in (2.1) with a method of lines approach, partitioning the temporal interval as  $0 = t_0 < \dots < t_n < \dots < t_{N_t} = T$ , and evaluate the spatial finite-element discretisation at the discrete points in time  $t_n$ , with the initial condition given by a spatial finite-element formulation at  $t_0$ . We begin by considering a Crank-Nicolson-type discretisation which, for linear problems, is equivalent to the lowest-order symplectic RK method, preserving quadratic invariants.

**Definition 2.3** (Finite-element discretization for linear KdV). Let  $U^j, W^j \in \mathbb{V}_q$  be given for  $j = 0, \dots, n$ . Then, we seek  $U^{n+1}, V, W^{n+1} \in \mathbb{V}_q$  such that

$$\begin{aligned} \int_{\Omega} \left( \frac{U^{n+1} - U^n}{\tau_n} + \mathcal{G}_h(V) \right) \phi \, dx &= 0 & \forall \phi \in \mathbb{V}_q \\ \int_{\Omega} \left( V - U^{n+\frac{1}{2}} - \mathcal{G}_h(W^{n+\frac{1}{2}}) \right) \psi \, dx &= 0 & \forall \psi \in \mathbb{V}_q \\ \int_{\Omega} (W^{n+1} - \mathcal{G}_h(U^{n+1})) \chi \, dx &= 0 & \forall \chi \in \mathbb{V}_q, \end{aligned}$$

where  $U^{n+\frac{1}{2}} := \frac{1}{2}(U^{n+1} + U^n)$  and  $W^{n+\frac{1}{2}} := \frac{1}{2}(W^{n+1} + W^n)$  for  $n = 0, \dots, N_t - 1$ . We define the initial data  $U^0 = \Pi u_0(x)$  where  $\Pi$  denotes the  $L_2$  projection into the finite-element space,  $\mathbb{V}_q$ , and we initialise  $W$  such that  $W^0 = \mathcal{G}_h(U^0)$  (as required for the conservation properties of the scheme [26, §4]). Note that only the intermediate value,  $V^{n+\frac{1}{2}}$ , is required for the scheme; while we could compute this from  $V^n$  and  $V^{n+1}$ ,

this does not change the conservative properties of the discretisation, so we neglect the time dependence in this term, noting that it arises implicitly through the dependence on  $U$  and  $W$ . In addition, we evaluate the third equation at  $t_{n+1}$  as, for momentum conservation, it is important to be able to reformulate a discrete difference of form

$$\int_{\Omega} \left( \frac{W^{n+1} - W^n}{\tau_n} - \mathcal{G}_h \left( \frac{U^{n+1} - U^n}{\tau_n} \right) \right) \chi \, dx = 0.$$

This finite element discretisation preserves fully discrete versions of mass, momentum and energy (see [26, §4]), which may be expressed as

$$\begin{aligned} \int_{\Omega} U^{n+1} \, dx &= \int_{\Omega} U^n \, dx \\ \int_{\Omega} \frac{1}{2} [U^{n+1}]^2 \, dx &= \int_{\Omega} \frac{1}{2} [U^n]^2 \, dx \\ \frac{1}{2} \int_{\Omega} [W^{n+1}]^2 - [U^{n+1}]^2 \, dx &= \frac{1}{2} \int_{\Omega} [W^n]^2 - [U^n]^2 \, dx. \end{aligned}$$

We write the complete finite-element solution at  $t = t_n$  as  $\mathbf{Z}^n = [U^n; V; W^n] \in \mathbb{V}_q^3$  through concatenating the solution. In turn, this allows us to define the discrete solution vector  $\mathbf{z}^n \in \mathbb{R}^{3(q+1)M_x}$  as the basis coefficients of  $\mathbf{Z}^n$ . We can then express these constraints by defining  $g_1(\mathbf{z}^n) = \int_{\Omega} U^n \, dx$ ,  $g_2(\mathbf{z}^n) = \int_{\Omega} \frac{1}{2} [U^n]^2 \, dx$ , and  $g_3(\mathbf{z}^n) = \frac{1}{2} \int_{\Omega} [W^n]^2 - [U^n]^2 \, dx$ . In order to explicitly write the constraints in terms of the vector  $\mathbf{z}^{n+1}$ , we define the vector  $\boldsymbol{\omega}(u) \in \mathbb{R}^{3(q+1)M_x}$  such that

$$\omega(u)_i := \int_{\Omega} \Psi_i^u \, dx,$$

where  $\Psi_i^u$  represents the  $i$ -th basis function for variable  $U$  in the trial space for  $\mathbf{Z} \in \mathbb{V}_q^3$ . Similarly, we define the mass matrices of the vector components

$$M(u)_{ij} := \int_{\Omega} \Psi_i^u \Psi_j^u \, dx \quad \text{and} \quad M(w)_{ij} := \int_{\Omega} \Psi_i^w \Psi_j^w \, dx.$$

We emphasise that both the vector  $\boldsymbol{\omega}(u)$  and these matrices are of dimension  $3(q+1)M_x$ , the same as our solution vector,  $\mathbf{z}^{n+1}$  (the complete discrete approximation). Indeed, we can rewrite our conservation laws in terms of dot products and inner products of these vector/matrices and  $\mathbf{z}^{n+1}$ , as

$$\begin{aligned} g_1(\mathbf{z}^{n+1}) &= \boldsymbol{\omega}(u)^T \mathbf{z}^{n+1} = \int_{\Omega} U^0 \, dx, \\ g_2(\mathbf{z}^{n+1}) &= \frac{1}{2} [\mathbf{z}^{n+1}]^T M(u) \mathbf{z}^{n+1} = \frac{1}{2} \int_{\Omega} [U^0]^2 \, dx, \\ g_3(\mathbf{z}^{n+1}) &= \frac{1}{2} [\mathbf{z}^{n+1}]^T M(w) \mathbf{z}^{n+1} - \frac{1}{2} [\mathbf{z}^{n+1}]^T M(u) \mathbf{z}^{n+1} = \frac{1}{2} \int_{\Omega} [W^0]^2 - [U^0]^2 \, dx. \end{aligned}$$

We note that the “local” expression of these conserved quantities is that  $g_{\ell}(\mathbf{z}^{n+1}) = g_{\ell}(\mathbf{z}^n)$  for  $\ell = 1, 2, 3$ ; however, we have iterated these laws back to the initial data, which shows that these values are constants, determined only by  $U^0$  and  $W^0$ .

To generalise the temporal discretisation used in (2.3) to arbitrarily high temporal order while preserving quadratic invariants, we use higher-order GLRK discretisations [21].

**Definition 2.4** (GLRK finite element discretisation for lKdV). Let  $s$  be the number of RK stages, and  $U^j, V^j, W^j \in \mathbb{V}_q$  be given for  $j = 0, \dots, n$ . The approximation  $U^{n+1}, V^{n+1}, W^{n+1}$  is given by seeking stage values  $K_U^i, K_V^i, K_W^i \in \mathbb{V}_q$  for  $i = 1, \dots, s$ , such that

$$\begin{aligned} \int_{\Omega} (K_U^i + \mathcal{G}_h(V_i^n)) \phi \, dx &= 0 & \forall \phi \in \mathbb{V}_q, 1 \leq i \leq s \\ \int_{\Omega} (V_i^n - U_i^n - \mathcal{G}_h(W_i^n)) \psi \, dx &= 0 & \forall \psi \in \mathbb{V}_q, 1 \leq i \leq s \\ \int_{\Omega} (W_i^n - \mathcal{G}_h(U_i^n)) \chi \, dx &= 0 & \forall \chi \in \mathbb{V}_q, 1 \leq i \leq s, \end{aligned}$$

where  $U_i^n = U^n + \tau_n \sum_{j=1}^s a_{ij} K_U^j$ ,  $V_i^n = V^n + \tau_n \sum_{j=1}^s a_{ij} K_V^j$ , and  $W_i^n = W^n + \tau_n \sum_{j=1}^s a_{ij} K_W^j$ . After solving for the stage values, the solution at  $t = t_{n+1}$  is constructed through

$$\begin{aligned} U^{n+1} &= U^n + \tau_n \sum_{i=1}^s b_i K_U^i, & V^{n+1} &= V^n + \tau_n \sum_{i=1}^s b_i K_V^i, \\ W^{n+1} &= W^n + \tau_n \sum_{i=1}^s b_i K_W^i. \end{aligned}$$

We note that, if  $U^n$ ,  $V^n$ , and  $W^n$  satisfy  $\int_{\Omega} (V^n - U^n - \mathcal{G}_h(W^n)) \psi \, dx = 0$  for all  $\psi$  and  $\int_{\Omega} (W^n - \mathcal{G}_h(U^n)) \chi \, dx = 0$  for all  $\chi$ , then the second two equations in (2.4) can be enforced directly on the stage values, rather than on the full stage approximations, and these relations will also hold at time-step  $n+1$ . These can be enforced at time-step 0 by requiring that  $W^0 = \mathcal{G}_h(U^0)$ , where  $U^0$  is the given initial data for  $U$  (typically,  $U^0 = \Pi u_0$ ), and that  $V^0 = U^0 + \mathcal{G}_h(W^0)$ .

When  $s = 1$ , Definition 2.4 is equivalent to the Crank-Nicolson scheme; however, we note that the discrete solution process is not identical, since the Crank-Nicolson scheme solves directly for  $U^{n+1}, V^{n+1}, W^{n+1}$ , while the one-stage Gauss-Legendre (implicit midpoint) scheme solves for the stage values, then updates  $U^n, V^n, W^n$  to get the values at the next time-step.

The conserved quantities for the higher-order scheme are unchanged and given by (2.1). These constraints are enforced in much the same way, except that the solution to the linear system  $\mathcal{A}\mathbf{x} = \mathbf{f}$  is no longer  $\mathbf{z}^{n+1}$ , the basis coefficients of  $\mathbf{Z}^{n+1}$ . Instead, we must accumulate the stage values encoded in  $\mathbf{x}$  to get  $\mathbf{z}^{n+1}$ , given by

$$\mathbf{z}^{n+1} = \mathbf{z}^n + \tau_n \sum_{i=1}^s b_i \mathbf{x}^i,$$

where  $\mathbf{z}^n$  is the solution at time  $t = t_n$  and  $\mathbf{x}^i$  is the restriction of  $\mathbf{x}$  to the  $i$ -th stage. With (2.1) in mind, an  $s$ -stage GLRK method exactly preserves the algebraic form of the constraints (2.1).

**2.2. Shallow water equations.** We next consider a two-dimensional domain, with  $\mathbf{x} \in \Omega = [0, X] \times [0, Y]$  and  $t \in [0, T]$ . On that domain, we consider  $\mathbf{u}(t, \mathbf{x}) \in \mathbb{R}^2$  representing a horizontal velocity and  $\rho(t, \mathbf{x}) \in \mathbb{R}$  a proxy for pressure, and define the linear rotating shallow water equations,

$$\begin{aligned} \mathbf{u}_t + f\mathbf{u}^\perp + c^2 \nabla \rho &= 0 \\ \rho_t + \nabla \cdot \mathbf{u} &= 0, \end{aligned}$$

where  $f$  is the Coriolis parameter,  $c^2$  is the gravitational acceleration times the mean layer thickness, and  $\mathbf{u}^\perp = \mathbf{e}_3 \times \mathbf{u}$ . We impose doubly periodic boundary conditions for both  $\mathbf{u}$  and  $\rho$  on  $\partial\Omega$ .

We use the discretisation from [14], which preserves many of the geometric properties of the shallow water equations on triangulations of  $\Omega$ . Letting  $H(\text{div}, \Omega)$  be the space of vector fields,  $\mathbf{u} \in (L^2(\Omega))^2$ , such that  $\nabla \cdot \mathbf{u} \in L^2(\Omega)$ , we consider approximating  $\mathbf{u}$  in the Raviart-Thomas space of degree  $q$ , denoted  $\text{RT}_q$ . (We note that, in our notation, the lowest-order Raviart-Thomas space is  $\text{RT}_1$ , and that the basis functions for  $\text{RT}_q$  are subsets of polynomials of degree at most  $q$ .) To represent  $\rho$ , we use discontinuous Lagrange elements of degree  $q-1$ , denoted again by  $\mathbb{V}_{q-1}$  (although we note that this is now the two-dimensional discontinuous Lagrange space on triangles). With these, and an integration-by-parts on  $\nabla \rho$ , the semi-discretised finite-element method seeks  $\mathbf{U} \in \text{RT}_q$  and  $P \in \mathbb{V}_{q-1}$  such that

$$\begin{aligned} \int_{\Omega} \mathbf{U}_t \cdot \phi + f\mathbf{U}^\perp \cdot \phi - c^2 P \nabla \cdot \phi \, dx &= 0 & \forall \phi \in \text{RT}_q \\ \int_{\Omega} P_t \psi + \nabla \cdot \mathbf{U} \psi \, dx &= 0 & \forall \psi \in \mathbb{V}_{q-1}. \end{aligned}$$

This scheme takes advantage of the discrete de Rham complex of finite-element exterior calculus [2, 13], with the property that for  $\mathbf{U} \in \text{RT}_q$ , we have  $\nabla \cdot \mathbf{U} \in \mathbb{V}_{q-1}$ . We note that [14] advocates for use of higher-order analogues of the BDFM<sub>1</sub> space in place of  $\text{RT}_q$ . This is necessary to preserve additional important invariants in the context of atmospheric dynamics, but not for the simpler invariants that we consider here.

We utilise Crank-Nicolson for our temporal discretisation. Due to the linear nature of the problem, the invariants will be quadratic, thus the temporal discretisation shall be conservative.

**Definition 2.5** (Finite element discretization for SWE). Let  $\mathbf{U}^j \in \text{RT}_q$ ,  $\mathbf{P}^j \in \mathbb{V}_{q-1}$  be given for  $j = 0, \dots, n$ , then we seek  $\mathbf{U}^{n+1} \in \text{RT}_q$  and  $\mathbf{P}^{n+1} \in \mathbb{V}_{q-1}$  such that

$$\begin{aligned} \int_{\Omega} \left( \frac{\mathbf{U}^{n+1} - \mathbf{U}^n}{\tau_n} \right) \cdot \phi + f \left[ \mathbf{U}^{n+\frac{1}{2}} \right]^{\perp} \cdot \phi - c^2 \mathbf{P}^{n+\frac{1}{2}} \nabla \cdot \phi \, dx &= 0 \quad \forall \phi \in \text{RT}_q \\ \int_{\Omega} \left( \frac{\mathbf{P}^{n+1} - \mathbf{P}^n}{\tau_n} \right) \psi + \nabla \cdot \mathbf{U}^{n+\frac{1}{2}} \psi \, dx &= 0 \quad \forall \psi \in \mathbb{V}_{q-1}, \end{aligned}$$

where  $\mathbf{U}^{n+\frac{1}{2}} = \frac{1}{2} (\mathbf{U}^n + \mathbf{U}^{n+1})$  and  $\mathbf{P}^{n+\frac{1}{2}} = \frac{1}{2} (\mathbf{P}^n + \mathbf{P}^{n+1})$ .

This finite-element discretisation conserves a plethora of geometric properties (cf., [14]). Here, we focus on the conservation laws for mass and energy, namely that

$$\int_{\Omega} \mathbf{P}^{n+1} \, dx = \int_{\Omega} \mathbf{P}^n \, dx$$

and

$$\frac{1}{2} \int_{\Omega} |\mathbf{U}^{n+1}|^2 + c^2 [\mathbf{P}^{n+1}]^2 \, dx = \frac{1}{2} \int_{\Omega} |\mathbf{U}^n|^2 + c^2 [\mathbf{P}^n]^2 \, dx,$$

respectively. As before, we define  $\mathbf{Z}^{n+1} = [\mathbf{U}^{n+1}; \mathbf{P}^{n+1}]$  and denote the solution vector in terms of the basis coefficients as  $\mathbf{z}^{n+1}$ . As we directly solve for  $\mathbf{z}^{n+1}$  in the Crank-Nicolson discretisation, we have  $\mathbf{z}^{n+1} = \mathbf{x}$ , the solution of  $\mathcal{A}\mathbf{x} = \mathbf{f}$ . To reformulate the constraints, we define the weight vector and mass matrices componentwise as

$$\omega(\rho)_i := \int_{\Omega} \Psi_i^{\rho} \, dx, \quad M(\mathbf{u})_{ij} := \int_{\Omega} \Psi_i^{\mathbf{u}} \cdot \Psi_j^{\mathbf{u}} \, dx, \quad M(\rho)_{ij} := \int_{\Omega} \Psi_i^{\rho} \Psi_j^{\rho} \, dx,$$

where the linear operators are formed through decomposing the trial and test functions in terms of their basis functions. We note that while these operators are formulated similarly to their analogues for the linear KdV equation, these are, in practice, quite different due to the differing natures of the basis functions. With these operators, we write the constraints on the underlying linear system as

$$\begin{aligned} g_1(\mathbf{z}^{n+1}) &= \omega(\rho)^T \mathbf{z}^{n+1} = \int_{\Omega} \mathbf{P}^0 \, dx \\ g_2(\mathbf{z}^{n+1}) &= \frac{1}{2} (\mathbf{z}^{n+1})^T M(\mathbf{u}) \mathbf{z}^{n+1} + \frac{c^2}{2} (\mathbf{z}^{n+1})^T M(\rho) \mathbf{z}^{n+1} = \frac{1}{2} \int_{\Omega} |\mathbf{U}^0|^2 + c^2 [\mathbf{P}^0]^2 \, dx, \end{aligned}$$

where the right-hand sides are, again, constants determined by the initial conditions.

**2.3. Heat equation.** Let  $u(t, \mathbf{x}) \in \mathbb{R}$  for  $\mathbf{x} \in \Omega = [0, 1] \times [0, 1]$  and  $t \in [0, 1]$ , then the heat equation may be written as

$$u_t - \Delta u = 0,$$

where, for simplicity, we employ Neumann boundary conditions in space. We consider a standard discretisation of the heat equation using conforming Lagrangian finite elements, writing the space of  $q$ -th order triangular Lagrangian elements over the domain  $\Omega$  as  $\mathbb{P}_q$ . The spatial finite-element semi-discretisation of (2.3) is then given by seeking  $u \in \mathbb{P}_q$  such that

$$\int_{\Omega} U_t \phi + \nabla U \cdot \nabla \phi \, dx = 0 \quad \forall \phi \in \mathbb{P}_q,$$

subject to some initial conditions  $U(0, \mathbf{x}) = \Pi u_0(\mathbf{x})$ . We again discretise temporally with Crank-Nicolson leading to the following fully discrete method.

**Definition 2.6** (Finite element discretization for the heat equation). Let  $U^j \in \mathbb{P}_q$  be given for  $j = 0, \dots, n$ , then we seek  $U^{n+1}$  such that

$$\int_{\Omega} \left( \frac{U^{n+1} - U^n}{\tau_n} \right) \phi + \nabla U^{n+\frac{1}{2}} \cdot \nabla \phi \, dx = 0 \quad \forall \phi \in \mathbb{P}_q,$$

where  $U^0 = \Pi u_0(\mathbf{x})$  and  $U^{n+\frac{1}{2}} = \frac{1}{2} (U^n + U^{n+1})$ .



The heat equation respects conservation of mass and a dissipation law, and its finite-element approximation preserves discrete counterparts of these; namely, the mass conservation law

$$\int_{\Omega} U^{n+1} dx = \int_{\Omega} U^n dx$$

and the dissipation law

$$\frac{1}{2\tau_n} \int_{\Omega} [U^{n+1}]^2 - [U^n]^2 dx = - \int_{\Omega} \nabla U^{n+\frac{1}{2}} \cdot \nabla U^{n+\frac{1}{2}} dx,$$

which can be rewritten as

$$\frac{1}{2} \int_{\Omega} [U^{n+1}]^2 + \frac{\tau_n}{4} [\nabla U^{n+1}]^2 + \frac{\tau_n}{2} \nabla U^{n+1} \cdot \nabla U^n dx = \frac{1}{2} \int_{\Omega} [U^n]^2 - \frac{\tau_n}{4} [\nabla U^n]^2 dx.$$

To reformulate mass conservation and energy dissipation in terms of the underlying linear system, we require the weight vector and mass matrix

$$\omega_i = \int_{\Omega} \Psi_i dx \quad \text{and} \quad M_{ij} = \int_{\Omega} \Psi_i \Psi_j dx,$$

in addition to the stiffness matrix  $L$  defined such that

$$L_{ij} = \int_{\Omega} \nabla \Psi_i \cdot \nabla \Psi_j dx.$$

We note that, while the mass conservation law can again be formulated in terms of only the initial condition, the dissipation law is more naturally expressed in terms of time-steps  $n$  and  $n+1$ . From the discrete solution  $\mathbf{z}^{n+1}$  to the Crank-Nicolson discretisation, we can express the constraints as

$$g_1(\mathbf{z}^{n+1}) = \boldsymbol{\omega}^T \mathbf{z}^{n+1} = \int_{\Omega} U^0 dx$$

$$g_2(\mathbf{z}^{n+1}) = \frac{1}{2} (\mathbf{z}^{n+1})^T M \mathbf{z}^{n+1} + \frac{\tau_n}{4} (\mathbf{z}^{n+1})^T L \mathbf{z}^{n+1} + \frac{\tau_n}{2} (\mathbf{z}^{n+1})^T L \mathbf{z}^n = \frac{1}{2} (\mathbf{z}^n)^T M \mathbf{z}^n - \frac{\tau_n}{4} (\mathbf{z}^n)^T L \mathbf{z}^n.$$

We note that  $g_2(\mathbf{z}^{n+1})$  is no longer a constraint in the form of  $g_2(\mathbf{z}^{n+1}) = g_2(\mathbf{z}^n)$ , since this represents a dissipation law, not a conservation law. While we write the algorithms below as if the constraints are always conservation laws, we note that the algorithm can, in fact, apply to any relation  $G(\mathbf{z}^{n+1}, \mathbf{z}^n) = 0$ . To express this concisely in what follows, we consider a generic linear algebra problem,  $\mathcal{A}\mathbf{x} = \mathbf{f}$ , coming from one of these discretisations, along with a list of  $c$  constraints to be satisfied by the discrete solution,  $\mathbf{x}$ , of the form  $g_i(\mathbf{x}) = v_i$  for  $1 \leq i \leq c$ , noting that all of the constraints above can be written in this form, for both the Crank-Nicolson discretisations (where  $\mathbf{x} = \mathbf{z}^{n+1}$ ) and the higher-order GLRK discretisations (where  $\mathbf{z}^{n+1}$  is assembled from  $\mathbf{x}$ , as in (2.1)).

### 3. STRUCTURE-PRESERVING KRYLOV METHODS

Krylov methods [20, 38] are iterative algorithms for approximating solutions to linear systems  $\mathcal{A}\mathbf{x} = \mathbf{f}$ , by generating approximations to  $\mathbf{x}$  in the Krylov space given by

$$\mathcal{K}_{\ell}(\mathcal{A}, \mathbf{r}_0) = \text{span} \{ \mathbf{r}_0, \mathcal{A}\mathbf{r}_0, \dots, \mathcal{A}^{\ell-1}\mathbf{r}_0 \},$$

where  $\mathbf{r}_0 = \mathbf{f} - \mathcal{A}\mathbf{x}_0$  is the initial residual associated with an initial guess,  $\mathbf{x}_0$ , for  $\mathbf{x}$ . There are multiple (overlapping) classifications of Krylov methods. Some aim to minimise some norm of the error associated with  $\mathbf{x}_{\ell} \in \mathcal{K}_{\ell}(\mathcal{A}, \mathbf{r}_0)$ , while others aim to enforce some orthogonality relationship between that error and the Krylov space itself. Most commonly used techniques can be considered in the first class. Amongst these, we can further distinguish between those that make use of short-term recurrences (e.g., conjugate gradients for symmetric and positive-definite matrices, or MINRES for symmetric systems), and those that form and store an explicit basis (usually orthogonal in some inner product) for the Krylov space, such as GMRES. While it may be possible to adapt our approach to any method that stores an explicit basis, we focus on adapting flexible GMRES (FGMRES) to preserve conservation laws of the approximate solutions generated by an iterative method.

We note that there exist two commonly used variants of the GMRES methodology, that differ in how preconditioners are incorporated. Standard GMRES aims to choose  $\mathbf{x}_{\ell}$  to minimise the residual,  $\mathbf{f} - \mathcal{A}\mathbf{x}_{\ell}$ ,



over the affine space  $\mathbf{x}_\ell = \mathbf{x}_0 + \delta\mathbf{x}_\ell$ , where  $\delta\mathbf{x}_\ell \in \mathcal{K}_\ell(\mathcal{A}, \mathbf{r}_0)$ . The standard approach is to use the Arnoldi algorithm to form an orthogonal basis for  $\mathcal{K}_\ell(\mathcal{A}, \mathbf{r}_0)$ , expressed as the range of the  $sd \times \ell$  matrix,  $Q_\ell$  (recall that  $\mathcal{A} \in \mathbb{R}^{sd \times sd}$ , where  $s$  is the number of Runge-Kutta stages, and  $d$  is the dimension of the spatial discretisation). Then, defining the  $(\ell + 1) \times \ell$  Hessenberg matrix,  $H_\ell$ , associated with the Arnoldi basis in  $Q_\ell$ , whose first column is  $\mathbf{r}_0$ , the problem of minimising  $\|\mathbf{f} - \mathcal{A}\mathbf{x}_\ell\|$  for  $\mathbf{x}_\ell = \mathbf{x}_0 + Q_\ell\mathbf{y}_\ell$  is equivalent to that of minimising  $\|\beta\mathbf{e}_{\ell+1} - H_\ell\mathbf{y}_\ell\|$ , for  $\beta = \|\mathbf{r}_0\|$  and  $\mathbf{e}_{\ell+1}$  the unit vector of length  $\ell + 1$  with first entry 1 and all other entries zero. Standard GMRES uses Householder transformations to iteratively compute a representation of the QR factorisation of  $H_\ell$  (updating that of  $H_{\ell-1}$ ) that allows us to compute the value of the norm at each step, then solve a triangular system for  $\mathbf{y}_\ell$  once a stopping criterion is satisfied (see [38] for full details). Left or right preconditioners can be incorporated by replacing the matrix  $\mathcal{A}$  with  $\mathcal{P}\mathcal{A}$  or  $\mathcal{A}\mathcal{P}$ , respectively, in the Arnoldi algorithm, to find  $\mathbf{y}_k$  that minimises either

$$\|\mathcal{P}\mathbf{f} - \mathcal{P}\mathcal{A}(\mathbf{x}_0 + Q_\ell\mathbf{y}_\ell)\|$$

for left preconditioning or

$$\|\mathbf{f} - \mathcal{A}(\mathbf{x}_0 + \mathcal{P}Q_\ell\mathbf{y}_\ell)\|$$

for right preconditioning.

For many problems, right preconditioning is preferable to left preconditioning, as it does not change the norm of the underlying minimisation problem, just the Krylov space over which we minimise, becoming  $\mathcal{K}(\mathcal{A}\mathcal{P}, \mathbf{r}_0)$ . When right-preconditioning with classical GMRES, however, we require  $\ell + 1$  applications of  $\mathcal{P}$  to compute  $\mathbf{x}_\ell$ , with  $\ell$  used to compute the basis for the Arnoldi space, and one more to compute  $\mathbf{x}_\ell = \mathbf{x}_0 + \mathcal{P}Q_\ell\mathbf{y}_\ell$  once  $\mathbf{y}_\ell$  is known. The flexible GMRES (FGMRES) variant removes this “extra” application of the preconditioner in favour of doubling the vector storage, to store both the standard orthogonal basis for the Krylov space,  $Q_\ell$ , and its preconditioned form,  $Z_\ell = \mathcal{P}Q_\ell$  (computed and stored columnwise within the preconditioned Arnoldi iteration). Then, we can compute  $\mathbf{x}_\ell = \mathbf{x}_0 + Z_\ell\mathbf{y}_\ell$  once  $\mathbf{y}_\ell$  is known. Unless the target computation is severely memory-limited, using FGMRES is generally preferred, particularly when the cost of preconditioner application is high (as it is in many cases when  $\mathcal{A}$  comes from the discretisation of coupled systems of PDEs). This also offers the flexibility to use different preconditioners at different inner iterations, with  $\mathcal{P}_\ell$  applied at step  $\ell$ , although we do not exploit this feature in what follows. For completeness, we sketch the FGMRES algorithm in Algorithm 1, albeit omitting the important details of the QR factorisation of  $H_\ell$ .

**Remark 3.1** (Restarting). For simplicity, we do not include restarting in any of the algorithms presented here, as it does not play a role in any of the numerical results. In many settings, however, particularly when the choice of optimal preconditioners is difficult, restarting is an important factor in limiting the memory consumption of GMRES-type algorithms. In Algorithm 1, restarting would take the form of an outer loop over all of the presented algorithm, looping until either convergence is achieved or some maximum number of restarts is reached. If convergence is not reached before  $\ell_{\max}$  steps, we compute  $\mathbf{x}_{\ell_{\max}}$  in Step 16 and use it to overwrite  $\mathbf{x}_0$  to restart the outer loop.

**3.1. A prototype for constrained GMRES.** The core idea of this paper is to constrain FGMRES such that desired properties of the discretisation are satisfied. This is achieved through modifying Line 13 in Algorithm 1. Instead of directly minimising the residual over the Krylov subspace, we pose a constrained minimisation problem, ensuring that the reconstructed solution,  $\mathbf{x}_\ell = \mathbf{x}_0 + Z_\ell\mathbf{y}_\ell$ , associated with the (constrained) minimiser,  $\mathbf{y}_\ell$ , satisfies the desired set of constraints.

That is, we replace Line 13 with a minimisation problem of the form

$$\mathbf{y}_\ell = \min_{\mathbf{y} \in \mathcal{Y}_\ell} \|\beta\mathbf{e}_{\ell+1} - H_\ell\mathbf{y}\|$$

$$\text{for } \mathcal{Y}_\ell = \left\{ \mathbf{y} \in \mathbb{R}^\ell \mid g_i(\mathbf{x}_0 + Z_\ell\mathbf{y}) = v_i \text{ for } 0 \leq i \leq \min(\ell - 1, c) \right\},$$

where we consider an additional input to the algorithm of  $\mathcal{C}_{\text{list}} = \{g_1, g_2, \dots, g_c\}$ , a list of constraints, each of form  $g_\ell(\mathbf{x}) = v_\ell$ .

In the general case (when  $\ell > c$ ), this can be thought of in terms of a nonlinear optimisation problem in  $\ell + c$  variables, with the  $c$  constraints imposed via Lagrange multipliers. In practice, we use the Python library SciPy, using the `optimize.minimize` function. This employs a sequential quadratic programming

---

**Algorithm 1:** FGMRES

---

```
Input:  $\mathcal{A}, \mathbf{f}, \mathbf{x}_0$  // Matrix, right-hand side, initial guess
       $\ell_{\max}$  // Maximum number of iterations
       $\mathcal{P}$  // Preconditioner (optional, defaults to identity matrix), may depend on iteration,  $\ell$ 
       $\epsilon$  // Convergence tolerance
Output:  $\mathbf{x}_\ell$  // Returns an approximation of the linear system

1  $\mathbf{r}_0 = \mathbf{f} - \mathcal{A}\mathbf{x}_0$ 
2  $\beta = \|\mathbf{r}_0\|$ 
3  $\mathbf{q}_1 = \mathbf{r}_0/\beta$ 
4 for  $\ell = 1, \dots, \ell_{\max}$  do // Loop over iterations
5    $\mathbf{z}_\ell = \mathcal{P}_\ell \mathbf{q}_\ell$ 
6    $\mathbf{q} = \mathcal{A}\mathbf{z}_\ell$ 
7   for  $i = 0, \dots, \ell + 1$  do // Arnoldi iteration
8      $h_{i\ell} = \mathbf{q}_i^T \mathbf{q}$ 
9      $\mathbf{q} = \mathbf{q} - h_{i\ell} \mathbf{q}_i$ 
10   $h_{\ell+1,\ell} = \|\mathbf{q}\|$ 
11  if  $h_{\ell+1,\ell} \neq 0$  then
12     $\mathbf{q}_{\ell+1} = \mathbf{q}/h_{\ell+1,\ell}$ 
13   $\mathbf{y}_\ell = \min_{\mathbf{y}} \|\beta e_{\ell+1} - H_\ell \mathbf{y}\|$  // Find minimiser in residual over Krylov space
14  if  $\|\beta e_{\ell+1} - H_\ell \mathbf{y}_\ell\| < \epsilon$  then
15    Break
16  $\mathbf{x}_\ell = \mathbf{x}_0 + Z_\ell \mathbf{y}_\ell$  // Assemble solution at current step
```

---

algorithm, SQSLP, which wraps the original (Fortran) implementation by Kraft [28]. In preliminary work, we also considered a Byrd-Omojokun Trust-Region SQP method [12, Section 15.4.2], as implemented in the `trust-constr` algorithm, but found this to be significantly less efficient when timing the results, likely because it does not allow us to directly provide gradients of the constraints. We note that this is substantially less efficient than the updating QR factorisation typically used for the Hessenberg matrix,  $H_\ell$ , in standard (F)GMRES. While it may be possible to optimize this solve in the case of only linear constraints (where the resulting first-order optimality condition is an  $(\ell + c) \times (\ell + c)$  linear system), we are unaware of any optimisations possible in the general case.

A crucial limitation of this methodology is that the vector subspace for the optimisation in (3.1) must be rich enough for a minimiser subject to the desired constraints to exist, which is not guaranteed for arbitrary choices of  $\mathbf{x}_0$ , particularly when  $\ell$  is small. Equation (3.1) mitigates this possibility by limiting the number of constraints enforced at step  $\ell$  to be no more than  $\ell$ . Of course, there is no guarantee that any given Krylov subspace will contain solutions which satisfy any given constraint; however, the constraints that we seek to impose here generally arise “naturally” within the system we are solving (in the sense that they are guaranteed to be satisfied by the exact solution of the underlying linear system), which gives some confidence that a constrained minimiser should exist, at least for sufficiently large  $\ell$ . With this in mind, we increase the number of constraints enforced as we loop through the iterations, starting with zero constraints and adding a new constraint each iteration. This procedure could be modified to allow for more or fewer constraints to be enforced in the early iterations, but preliminary experiments showed that adding one per iteration was sufficient for the majority of the test cases considered. We note that directly substituting (3.1) for Line 13 in Algorithm 1 implicitly assumes that the stopping criterion will not be satisfied until  $\ell \geq c$ . While this was true in practice in all experiments considered herein, it could easily be made an explicit condition on Line 15 if needed.

**3.2. Practical implementation of CGMRES.** Even when the Krylov space is rich enough such that a constrained minimiser exists for (3.1), the computational cost of finding such minimiser is substantially higher than that of the usual updating QR factorisation used in (F)GMRES. Indeed, performing the constrained

solves can be particularly expensive when the Krylov space is small, as significant effort can be required to find (or fail to find) a constraint-satisfying solution. Taken together, these suggest that a practical implementation of the constrained GMRES approach should be one where the use of constrained solves is avoided unless we are close enough to solution that the effort is worthwhile. One excellent indicator of whether or not this computational cost is worth expending is the size of the *unconstrained* residual, noting that we still use a residual-based stopping tolerance on constrained GMRES and that the residual in the constrained solution cannot be smaller than that in the unconstrained solution. Since the norm of the unconstrained residual can be computed at relatively low cost, this leads to an effective strategy for avoiding the nonlinear solve until we are close to convergence. In fact, a regular FGMRES routine could be used until this point, giving residual norm estimates from the standard approach using QR factorisation of the Hessenberg systems at no additional cost.

This approach is presented in Algorithm 2. Here, in addition to the standard residual-norm stopping parameter,  $\epsilon$ , we require a second tolerance,  $\mathcal{E}$ , to determine whether we are “close enough” to convergence to make enforcing the constraints in the solve worthwhile. An important practical question is, of course, how to choose the second parameter,  $\mathcal{E}$ . We note that we choose to structure the algorithm so that the decision to impose constraints is based on already computed information, at step  $\ell - 1$ . Thus, we view  $\mathcal{E}$  as being how close to convergence we expect to be at the iteration *prior* to satisfying the convergence criterion, so that we aim to perform only a single constrained solve. Thus,  $\mathcal{E}/\epsilon$  should be approximately the residual reduction per iteration expected from the unconstrained (but preconditioned) iteration, so that we only execute the solve on Line 16 once (assuming we can find a constraint-satisfying solution with similar overall residual reduction). For the systems considered here, we generally take  $\mathcal{E} = 10\epsilon$ , although we note that different choices could easily be justified, and that the interplay between constraints and residual minimisation in any particular problem may drive other choices (in particular in cases where the constrained residual norm is much larger than its unconstrained counterpart).

**Remark 3.2** (Restarting with constraints). As above, we do not explicitly include restarting in Algorithm 2, but note that it could be included as an additional “outer” loop. However, we also note a potential complication when restarting. As noted above, it can be difficult to enforce constraints when the Krylov space is too small. Thus, when we are close to convergence, it may be quite disadvantageous to restart, since we throw away a “rich” Krylov space over which we could effectively enforce the constraints and restart from a low-dimensional Krylov space, where enforcing constraints may be quite difficult. This issue did not impact the numerical results reported below in section 4; however, we expect that further attention to these details may be needed if the CGMRES methodology is applied in combination with problems and preconditioners for which restarting is commonplace. As written, Algorithm 2 suggests imposing the constraints at the end of each restart cycle (the outer loop that is implicitly there) and again at convergence in the inner loop. In practice, it is probably most useful to only enforce constraints once one is near convergence, provided the Krylov space is rich enough to expect success.

**Remark 3.3** (Additional computational cost). While the exact cost of including and enforcing the constraints is highly problem dependent, we generally expect these to increase the cost of the algorithm. Within this work, we exclude problem-specific optimisations and focus on constraints that can be expressed in the form

$$\mathbf{x}_\ell^T \mathcal{M} \mathbf{x}_\ell + \mathbf{x}_\ell^T \mathbf{v} + c = 0,$$

for  $\mathcal{M} \in \mathbb{R}^{sd \times sd}$ ,  $\mathbf{v} \in \mathbb{R}^{sd}$  and constant  $c$ , where  $sd$  is the dimension of the underlying linear system  $\mathcal{A}\mathbf{x} = \mathbf{f}$ . We note here that (3.3) is the general form of a conserved quantity for linear problems, but that more general constraints might be of interest for broader classes of PDEs. As written in theorem 3.3, the evaluation of this constraint has a cost of  $\mathcal{O}(sd)$ , assuming a sparse constraint matrix,  $\mathcal{M}$ . However, since  $\mathbf{x}_\ell = \mathbf{x}_0 + Q_\ell \mathbf{y}_\ell$  for  $\mathbf{y}_\ell \in \mathbb{R}^\ell$ , with  $\ell \ll sd$ , we can greatly reduce this cost, by precomputing various products with  $\mathbf{x}_0$  and  $Q_\ell$ . Rewriting (3.3), we have

$$\mathbf{y}_\ell^T (Q_\ell^T \mathcal{M} Q_\ell) \mathbf{y}_\ell + \mathbf{y}_\ell^T (2Q_\ell^T \mathcal{M} \mathbf{x}_0 + Q_\ell^T \mathbf{v}) + (\mathbf{x}_0^T \mathcal{M} \mathbf{x}_0 + \mathbf{x}_0^T \mathbf{v} + c) = 0,$$

noting that, in general,  $Q_\ell^T \mathcal{M} Q_\ell$  will be a dense matrix even if  $\mathcal{M}$  is sparse. Thus, we can evaluate the reduced constraint at a cost of  $\mathcal{O}(\ell^2)$ , for computing the inner product in the first term, plus an  $\mathcal{O}(\ell)$  cost for

---

**Algorithm 2:** Optimised constrained GMRES
 

---

```

Input:  $\mathcal{A}, \mathbf{f}, \mathbf{x}_0$  // Matrix, right-hand side, initial guess
           $\ell_{\max}$  // Maximum number of iterations
           $\mathcal{P}$  // Preconditioner (optional, defaults to identity matrix), may depend on iteration,  $\ell$ 
           $\epsilon$  // Convergence tolerance
           $\mathcal{C}_{\text{list}} = \{g_1, g_2, \dots, g_c\}$  // List of constraints of form  $g_\ell(\mathbf{x}) = v_\ell$ 
           $\mathcal{E}$  // Tolerance to check constraint enforcement, defaults to  $10\epsilon$ , must have  $\epsilon \leq \mathcal{E}$ 

Output:  $\mathbf{x}_\ell$  // Returns an approximation of the linear system

1  $\mathbf{r}_0 = \mathbf{f} - \mathcal{A}\mathbf{x}_0$ 
2  $\beta = \|\mathbf{r}_0\|$ 
3  $\mathbf{q}_1 = \mathbf{r}_0/\beta$ 
4 for  $\ell = 1, \dots, \ell_{\max}$  do // Loop over iterations
5    $\mathbf{z}_\ell = \mathcal{P}_\ell \mathbf{q}_\ell$ 
6    $\mathbf{q} = \mathcal{A}\mathbf{z}_\ell$ 
7   for  $i = 0, \dots, \ell + 1$  do // Arnoldi iteration
8      $h_{i\ell} = \mathbf{q}_i^T \mathbf{q}$ 
9      $\mathbf{q} = \mathbf{q} - h_{i\ell} \mathbf{q}_i$ 
10   $h_{\ell+1,\ell} = \|\mathbf{q}\|$ 
11  if  $h_{\ell+1,\ell} \neq 0$  then
12     $\mathbf{q}_{\ell+1} = \mathbf{q}/h_{\ell+1,\ell}$ 
13  if  $\|\beta e_\ell - H_{\ell-1} \mathbf{y}_{\ell-1}\| > \mathcal{E}$  and  $\ell < \ell_{\max}$  then // If far from tolerance and  $\ell \neq \ell_{\max}$ , use FGMRES
14     $\mathbf{y}_\ell = \min_{\mathbf{y}} \|\beta e_{\ell+1} - H_\ell \mathbf{y}\|$ 
15  else
16     $\mathbf{y}_\ell = \min_{\mathbf{y}} \|\beta e_{\ell+1} - H_\ell \mathbf{y}\|$  subject to the constraints  $\{g_1, \dots, g_c\}$  // If close to tolerance or
     $\ell = \ell_{\max}$ , use constrained solve
17    if constrained solve fails then
18      Go to line 14
19    if  $\|\beta e_{\ell+1} - H_\ell \mathbf{y}_\ell\| < \epsilon$  then
20      Break
21  $\mathbf{x}_\ell = \mathbf{x}_0 + Z_\ell \mathbf{y}_\ell$  // Assemble solution at current step
  
```

---

the dot product in the second. The cost of evaluating the Jacobian of the constraint is the same. However, in order to achieve this, we must precompute several terms. Multiplying the sparse matrix  $\mathcal{M}$  by the dense matrix  $Q_\ell$  has  $\mathcal{O}(sd\ell)$  cost ( $\mathcal{O}(1)$  cost for each entry in the resulting  $sd \times \ell$  matrix), so computing  $Q_\ell^T \mathcal{M} Q_\ell$  has cost  $\mathcal{O}(sd\ell^2)$ , and this is the dominant cost in precomputing the terms in the reduced constraint in (3.3). For perspective, this is the same cost as computing the Hessenberg system for the  $\ell$ -dimensional Krylov space in the Arnoldi algorithm. In particular, when  $\ell$  is small, this cost is typically dominated by the cost of the matrix-vector product and preconditioner applications in GMRES. We report details on practical (measured) computational costs in Section 4, showing that this cost is not trivial but, at the same time, does not dominate the computation.

**Remark 3.4** (Nonlinear iterative solvers). Extending this approach to nonlinear PDEs is slightly more invasive but still feasible. Here, we envision a Newton-Krylov approach, where the nonlinear equation for  $\mathbf{z}^{n+1}$  is linearised via Newton's method, and the successive linearisations are solved using FGMRES. In this setting, the solution of the linear system  $\mathcal{A}\mathbf{x} = \mathbf{f}$  represents the update to the current approximate solution of the nonlinear system, and a standard Newton linesearch method, used to improve robustness and efficiency of the nonlinear solve, updates the current approximation by computing  $\mathbf{z}^{n+1} = \mathbf{z}^n + \omega \mathbf{x}$ , with parameter  $\omega$  chosen to minimize (in some sense) the nonlinear residual norm along the line defined by  $\mathbf{z}^n$

and  $\mathbf{x}$ . Since this weight is not known before we solve for  $\mathbf{x}$ , it is difficult to compute updates that ensure that the solution of the nonlinear equation stays on the constraint.

While we do not implement and explore such methods here, we note that a similar strategy to the above may be mimicked in this case. Close to (nonlinear) convergence, it is typical to see the weight chosen by linesearch algorithms approach unit step size,  $\omega \rightarrow 1$ . Thus, it is possible to construct a constrained Newton-Krylov method that iterates using standard Newton iterations (with inexact solves, such as using the Eisenstat-Walker criteria [15], and linesearches) until suitably close to convergence such that fixing the step size to be one is reasonable. Then, the constrained GMRES algorithm can be applied to solve subsequent linearisations (ideally only the final linearisation) with constraints adapted to be posed on the (updated) nonlinear solution, now of the form  $\mathbf{z}^{n+1} = \mathbf{z}^n + \mathbf{x}$ , rather than directly on the solution,  $\mathbf{x}$ , of the Jacobian system.

#### 4. NUMERICAL EXPERIMENTS

Here we apply the methodology discussed in Section 3 for the problems and discretisations discussed in Section 2, highlighting the potential benefits and pitfalls when incorporating geometric constraints into linear solvers. Our implementation can be found in [27], making use of the Firedrake and Irksome libraries for the spatial and temporal discretisations [16, 36]. The specific versions of the Firedrake software used are recorded here [48]. All results presented here, including timings, have been computed on a single Xeon 2.4 GHz CPU core, with access to 128 GB of memory.

**4.1. Linear KdV.** Recall the discretisation of the linear KdV equation discussed in Section 2.1. We begin by solving the finite element approximation over a single time step subject to the initial condition

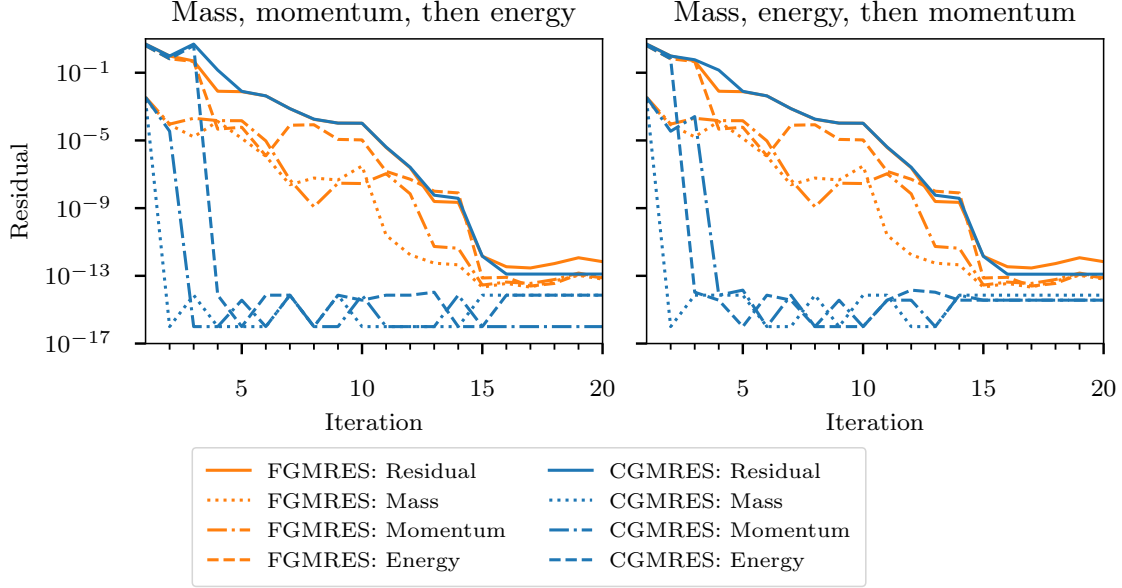
$$U^0 = \sin(\alpha x) + 1,$$

where  $\alpha = \frac{\pi}{5}$ . Note that we specifically choose  $U^0$  to not have zero mean, as zero-mean solutions can achieve conservation of mass automatically when using standard FGMRES with a zero-mean initial guess, as shown in [7, Section 3.3].

In Figure 1, we compare solutions generated using the CGMRES algorithm proposed in Section 3.1 against those generated with classical FGMRES, exploring the effects of the ordering in which the constraints are enforced with the Crank-Nicolson temporal discretisation (2.3). Here, we run both solvers for 20 iterations, to compare histories of residual norm reduction and constraint satisfaction. In both cases considered, we notice that the residual norm when using CGMRES is slightly larger than that with FGMRES for a few early iterations, while that with FGMRES is slightly larger than that with CGMRES near convergence. At convergence, we note that residuals are well below discretisation error for this system for both methods. In contrast, the conserved quantities are quickly enforced to the level of machine precision for the CGMRES solution while they decrease at the same rate as the residual norm for classical FGMRES. Interestingly, we note that if we constrain mass, then energy, and then momentum, our algorithm successfully finds constrained solutions at every step, as shown at right of Figure 1, with a steady decrease in the CGMRES residual norm and machine-precision errors in mass from the second iteration onwards, in energy from the third iteration onwards, and in momentum from the fourth iteration onwards. However, if we constrain mass, then momentum, then energy, the constrained solve on the third iteration leads to an increase in the residual norm when we impose all three constraints for the first time. We expect that this is due to the Krylov space not yet being rich enough to allow a good solution that satisfies all three constraints. As we continue to iterate, however, and the space over which we minimise grows, the constraints are more easily satisfied by the approximate solution and the residual norm for CGMRES decreases as expected. Note that if, instead of running a fixed number of iterations, we terminate the linear solvers at a typical residual-norm stopping tolerance of  $\epsilon = 10^{-6}$ , CGMRES performs comparably to FGMRES in both cases in terms of the residual norm, and allows us to enforce all constraints to the level of machine precision.

In addition to understanding the convergence of the iterative linear solvers over a single solve, it is crucial to understand how these algorithms impact simulations as they propagate approximate solutions over time. With this in mind, we use a standard stopping tolerance, of a residual norm reduction to  $\epsilon = 10^{-6}$  as the stopping criterion for each time step, and experiment with the more practical algorithmic alternative in Algorithm 2. Figure 2 presents two experiments. At left, we consider the time evolution using a zero initial

FIGURE 1. A comparison between CGMRES as proposed in Section 3.1 and FGMRES with no preconditioner. Here, the linear system we solve corresponds to the finite element scheme for linear KdV (2.3) where  $\tau = 0.01$ ,  $M_x = 50$  and the spatial degree is  $q = 1$ . We initialise  $U^0$  as given by (4.1) and solve for  $(U^1, V, W^1)$ . We take an initial guess for both linear solvers of  $\mathbf{x}_0 = \mathbf{0}$  and solve CGMRES subject to the constraints (2.1), varying the order in which the constraints are enforced.



guess for each time step. At right, we use the solution from the previous time step as the initial guess. As shown in [7, Section 3.3], using the solution from the previous time step leads to automatic conservation of mass, since we use the unpreconditioned algorithms here. Thus, when we impose the constraints on CGMRES in this case, we only impose constraints on momentum and energy, since the conservation of mass constraint is already satisfied. We observe in Figure 2 that all invariants are preserved to near machine precision by CGMRES. For standard FGMRES, on the other hand, we see that while mass is constrained to a relatively high tolerance in both cases, both momentum and energy deviate up to the order of the solver tolerance.

As discussed in Section 2.1, the methodology proposed here can be used for both Crank-Nicolson and the higher-order GLRK discretisations given in Definition 2.4. Next, we consider performance as we increase the temporal and spatial order, for a problem posed on a larger domain and discretised with more points in space. As is typical with any discretised PDE, increasing the order of and number of points in the discretisation also increases the condition number of the linear system to be solved, to the point where effective convergence of GMRES-like methods requires the use of a preconditioner. Here, since we discretise a one-dimensional PDE, we can make use of a simple preconditioner, such as the incomplete LU (ILU) factorisation of the system. Here, we make use of the ILU implementation provided by SuperLU [31, 32], through its interface to SciPy [45], using a supernodal ILUTP algorithm with drop tolerance  $10^{-4}$  and fill ratio upper bound of 10, given by the call

$$\mathcal{P} = \text{scipy.sparse.linalg.spilu}(A, \text{drop\_tol} = 10^{-4}, \text{fill\_factor} = 10).$$

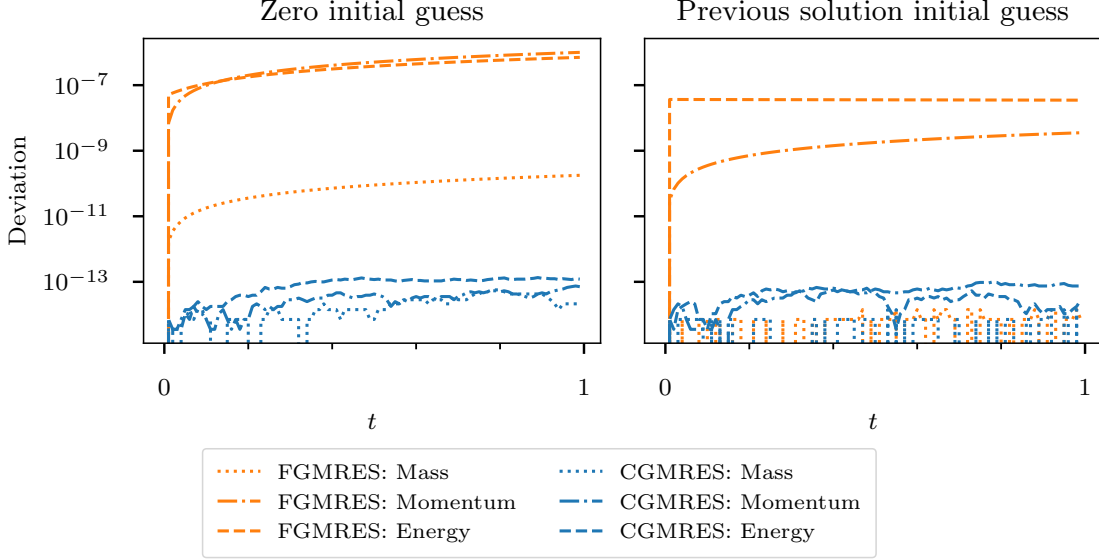
Simulating the trigonometric wave

$$u(t, x) = \sin(\alpha(x - (1 - \alpha^2)t)) + 1,$$

with  $\alpha = \frac{\pi}{5}$  over  $t \in [0, 1]$ ,  $x \in [0, 40]$ , for FGMRES, CGMRES, and exact linear solvers, we obtain Figure 3, showing the  $L_2$  error in the numerical solution at each time step, with  $\tau = 0.1$ . We note here that we



FIGURE 2. The deviation in mass, momentum and energy over time for the finite element scheme for linear KdV (2.3) where  $\tau = 0.01$ ,  $M_x = 50$ ,  $T = 1$  and the degree is  $q = 1$ , using the linear solvers FGMRES and CGMRES as described by Algorithm 1 and 2, respectively. Here, we fix  $\epsilon = 10^{-6}$  and constrain CGMRES by (2.1) with  $\mathcal{E} = 10\epsilon$ . We initialise  $U^0$  as given by (4.1) and solve iteratively for  $(U^{N_t}, V^{N_t}, W^{N_t})$ . At left, we present results for all three constraints using a zero initial guess for the linear solvers at each time step. At right, we present results for all three constraints using the solution from the previous time step as the initial guess at each time step, but only enforcing constraints on momentum and energy in CGMRES.



have greatly increased both the size of the spatial domain and the number of points used to discretise it, in comparison to the previous example. Note, however, that the spatial  $L_2$  error in the discretisation cannot scale better than  $(X/M_x)^{q+1}$  (as degree  $q$  polynomials are used) while the temporal error for an  $s$ -stage GLRK method should scale like  $\tau^{2s}$ , so we use slightly higher order spatial discretisations than temporal ones. For each discretisation, we plot the error observed using an exact solver for each timestep (LU factorisation), preconditioned FGMRES, and preconditioned CGMRES. We observe that CGMRES consistently outperforms FGMRES in this simulation, but remains less accurate than the exact solver. In fact, the solution error using FGMRES can be larger than that of solving the next lower-order discretisation using the exact solver, while CGMRES generally yields errors between those from the exact solver at the same order and at one order lower.

**4.2. Shallow water equations.** Here, we consider (2.2) with  $c = 1$  and  $f = 0.1$  over the domain  $t \in [0, 10]$ ,  $\mathbf{x} \in [0, 40] \times [0, 40]$ , where space is doubly periodic. We initialise our simulations with zero velocity and a Gaussian pressure distribution,

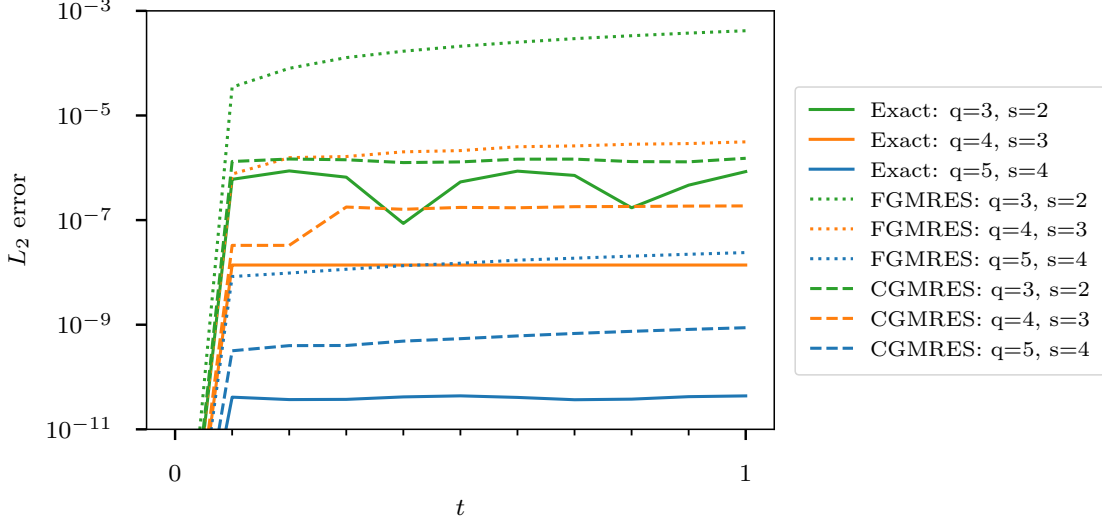
$$U^0 = \mathbf{0}$$

$$P^0 = 10 \exp \left( -\frac{(x-20)^2 + (y-20)^2}{20^2} \right).$$

In Figure 4, we again compare CGMRES against FGMRES in terms of residual norm and the preservation of conserved quantities, for degree  $q = 1$  and  $q = 2$ , over 20 iterations. We note that the conserved quantities converge at the same rate as the residual with FGMRES, whereas we are able to preserve both invariants at



FIGURE 3. The error propagation over time using direct linear solvers, FGMRES and CGMRES using an  $s$  stage GLRK temporal discretisation and the order  $q$  spatial discretisation (2.4) simulating (4.1). We fix  $\tau = 0.1$ ,  $M_x = 400$ , and vary the solver tolerance  $\epsilon$  to be  $10^{-3}$ ,  $10^{-5}$  and  $10^{-7}$ , respectively, as we increase the order of the method. Further, we precondition by (4.1) and initialise the linear solvers with either the stage values on the previous step, or a tiling of the initial data (for the first step).

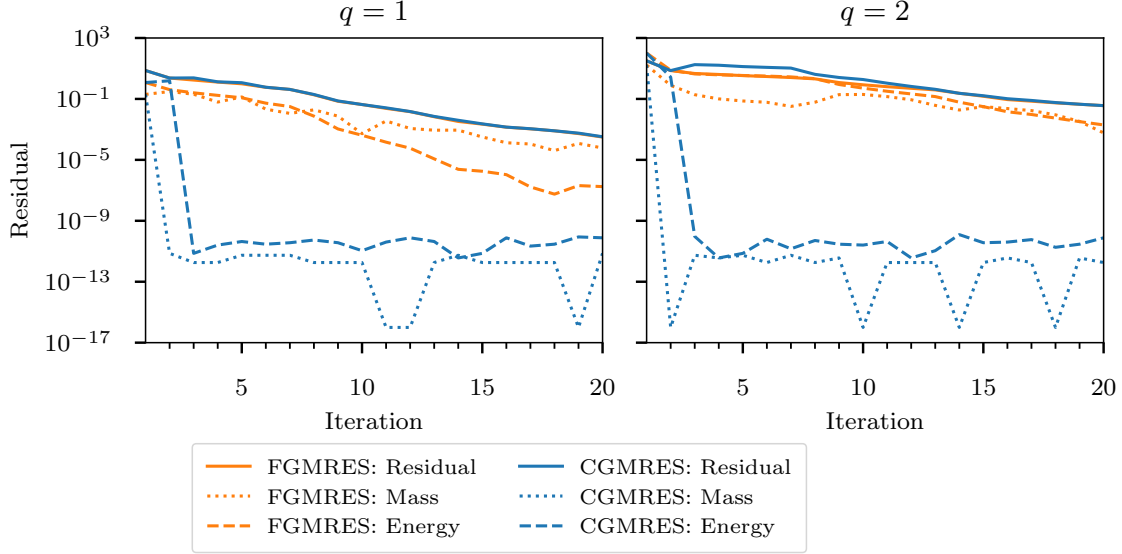


the level of machine precision for all iterations after the third using CGMRES. As for linear KdV, for early iterations, we see that the residual for CGMRES is slightly larger than that for FGMRES, but that the two residuals quickly become comparable. For higher polynomial degree the convergence of both iterations is significantly slower, as is typical. While we do not consider this in Figure 4, convergence could be improved by either improving the initial guess (we use a zero initial guess here, for illustration), or by the use of a suitable preconditioner.

As for linear KdV, we next study the effect of the different linear solvers for many timesteps, using a typical GMRES stopping tolerance of  $\epsilon = 10^{-6}$ . We consider the same problem as above, with  $\tau = 0.1$  and  $q = 1$ . As above, Figure 5 presents results for both a zero initial guess and using the solution from the previous time step as the initial guess at each time step, showing that mass is conserved equally well in the latter case. In Figure 5, we observe that CGMRES accurately preserves the conservation laws well below the linear solver tolerance over long time, while energy conservation using FGMRES appears limited to that given by the solver tolerance, as is mass conservation when using a zero initial guess. Here, we do not have an analytical solution for comparison of accuracy between the two solution schemes.

Table 1 presents computational times for both FGMRES and CGMRES, using the same ILU preconditioner as considered above, but with drop tolerance set to  $10^{-2}$  instead of  $10^{-4}$ . We note that ILU is a rather expensive, but effective, preconditioner for this case, with the preconditioner setup time being, by far, the dominant time of the computation. For these parameters, we see (as expected) some growth in the number of iterations as  $M_x$  increases, leading to faster-than-linear growth in time-to-solution with problem size (which is proportional to  $M_x^2$ ). For each iteration of CGMRES, we time the cost per iteration, measuring the sum of the preconditioner application, matrix-vector product, Arnoldi orthogonalisation and solution of the Hessenberg system for the minimiser over the Krylov space. This is reported as  $\mathcal{T}_s$ , the average time for iterations in which constraints are not imposed, and  $\mathcal{T}_c$ , the average time for iterations in which the constraints are imposed. Additionally, we measure the cost of projecting the constraints onto the Krylov space (see Remark 3.3), again averaged over all constrained iterations, reported as  $\mathcal{T}_{\text{overhead}}$  in Table 1. For

FIGURE 4. A comparison between CGMRES as proposed in Section 3.1 and FGMRES for the linear shallow water equations. Here, the linear system corresponds to the numerical approximation (2.5) with  $\tau = 0.1$ ,  $M_x = 50$ , and variable degree  $q$  and the constraints are described by (2.1). We initialise  $\mathbf{U}^0$  and  $\mathbf{P}^0$  with (4.2) and solve for  $(\mathbf{U}^1, \mathbf{P}^1)$ . Further, we specify the initial guess for our linear solvers to be  $\mathbf{x}_0 = \mathbf{0}$ .



the largest values of  $M_x$  reported in the table, we see that the difference between the total FGMRES and CGMRES solve times is almost exactly equal to the cost of assembling the constraints, which is bounded by about twice the average cost of a single iteration of CGMRES. We note that our implementation of FGMRES does not implement the usual updating-QR factorisation approach to solving the Hessenberg system but, instead, uses the same `scipy.optimize.minimize` command to solve the system as in the constrained case, just without imposing the constraints. We have compared timings to those of a more standard FGMRES, as implemented in `PyAMG` [3] (noting that `SciPy` does not provide an FGMRES function), and found that our approach is slightly faster, at least for the small Krylov spaces we have used for comparison. We also note that, as expected, the convergence of GMRES preconditioned by ILU suffers as the problem size gets larger and the convergence tolerance gets stricter. Thus, while the added cost of CGMRES over FGMRES is noticeable in these examples (20-30% for  $M_x = 256$  and 512), this cost can clearly pay off when “regular” FGMRES requires many more iterations to enforce the constraints to suitable tolerances than are needed for the expected/desired residual reduction.

**4.3. Heat equation.** Recall the heat equation and associated discretisation discussed in Section 2.3. Experimentally, we consider a single time step with initial condition given by

$$U^0 = \Pi \left( 10^3 \left[ (x(x-1))^5 + (y(y-1)^6) \right] \right),$$

over the domain  $t \in [0, 1]$ ,  $\mathbf{x} \in [0, 1] \times [0, 1]$ , where  $\Pi$  is the  $L_2$  projection into the finite element space. Spatially, we employ Neumann boundary conditions. Due to the poor conditioning of the problem, we expect unpreconditioned iterative solvers to be slow to converge. With this in mind, we seek to use an effective preconditioner in the iteration. Unsurprisingly, performance using the ILU preconditioner deteriorates significantly when we increase problem size. Thus, for a timing and scaling study, we consider a much more robust preconditioning framework for the heat equation, that of Ruge-Stüben algebraic multigrid [10, 37, 42].

Multigrid methods [11, 44] are widely recognised as among the most efficient families of preconditioners for elliptic PDEs and for simple time discretisations of parabolic PDEs (although they can be readily adapted for

FIGURE 5. The deviation in mass and energy over time for the finite element scheme for the shallow water equations (2.5), with  $\tau = 0.1$ ,  $T = 10$ ,  $M_x = 50$ , and  $q = 1$ , using the linear solvers FGMRES and CGMRES as described by Algorithms 1 and 2, respectively. We constrain CGMRES by (2.1) and set  $\epsilon = 10^{-6}$  and  $\mathcal{E} = 10\epsilon$ . We initialise  $\mathbf{U}^0$  and  $\mathbf{P}^0$  with (4.2) and solve iteratively for  $(\mathbf{U}^{N_t}, \mathbf{P}^{N_t})$ . At left, we present results for both constraints using a zero initial guess for the linear solvers at each time step. At right, we present results for both constraints using the solution from the previous time step as the initial guess at each time step, but only enforcing the constraint on energy in CGMRES.

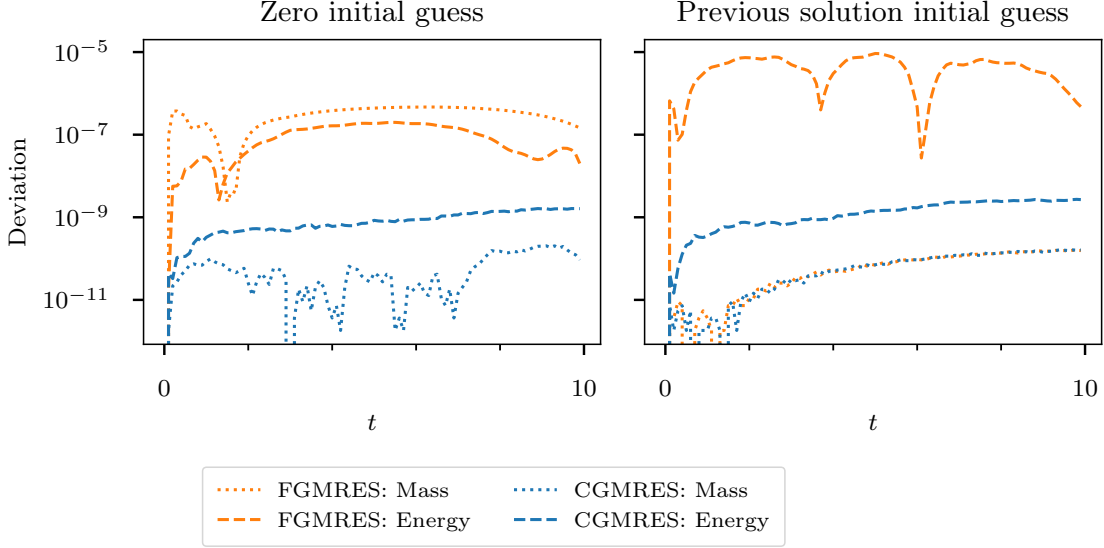


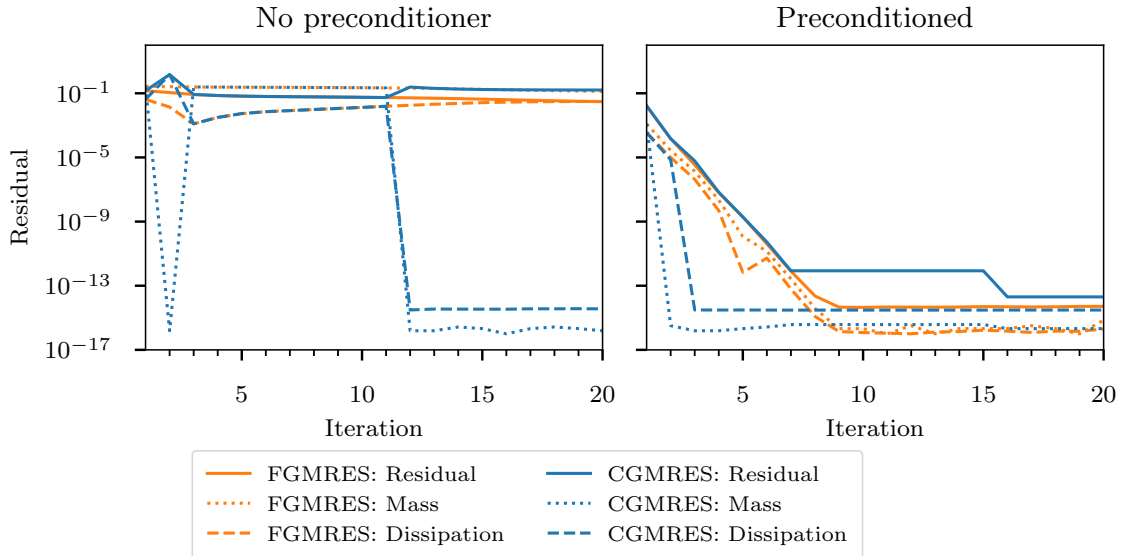
TABLE 1. Computational times for a single solve of the linear shallow water equations (2.5) preconditioned by (4.1) for variable spatial mesh resolutions  $M_x$ , with  $\tau = 0.1$ ,  $\epsilon = 10^{-7}$ ,  $\mathcal{E} = 10\epsilon$  and a zero initial guess for  $\mathbf{x}_0$ . We present the preconditioner assembly time (in seconds)  $\mathcal{T}_{\mathcal{P}}$ , total run time of FGMRES (as described in Algorithm 1)  $\mathcal{T}_{\text{gmres}}$ , total run time of CGMRES (as described in Algorithm 2)  $\mathcal{T}_{\text{cgmres}}$ , and total number of iterations for both FGMRES and CGMRES (which are the same in this example). We further break down the costs within CGMRES, writing  $\mathcal{T}_s$  as the average run time for an unconstrained iteration,  $\mathcal{T}_{\text{overhead}}$  as the average computational overhead (per constrained iteration) required to assemble the constraints, and  $\mathcal{T}_c$  as the constrained iteration cost. Here,  $\#(\mathcal{T}_c)$  denotes the number of constrained iterations of CGMRES.

$M_x$	32	64	128	256	512
$\mathcal{T}_{\mathcal{P}}$	4.18e-02	1.63e-01	8.96e-01	5.26e+00	3.07e+01
$\mathcal{T}_{\text{gmres}}$	1.18e-02	4.42e-02	2.08e-01	1.09e+00	7.03e+00
$\mathcal{T}_{\text{cgmres}}$	2.24e-02	7.90e-02	5.50e-01	1.38e+00	8.48e+00
Iterations	6	6	6	7	9
$\mathcal{T}_s$	2.31e-03	7.43e-03	3.40e-02	1.51e-01	7.64e-01
$\mathcal{T}_{\text{overhead}}$	3.53e-03	1.25e-02	4.84e-02	2.90e-01	1.43e+00
$\mathcal{T}_c$	6.95e-03	2.70e-02	3.27e-01	1.63e-01	8.41e-01
$\#(\mathcal{T}_c)$	1	1	1	1	1

more complex problems and discretisations; cf. [1, 16]), combining fine-scale relaxation schemes with coarse-level correction. For many problems, *geometric* multigrid methods, where the multigrid hierarchy is created using uniform refinement of structured grids with geometric (e.g., piecewise linear) grid-transfer operators, are the most efficient approaches. However, *algebraic* multigrid methods offer black-box solvers that can be easily applied based on the system matrix alone, without appealing to any geometric information about the underlying discretisation or meshes. Here, we use the implementation of Ruge-Stüben algebraic multigrid (AMG) with default parameters from PyAMG [3], determining coarse grids using the first pass of the original Ruge-Stüben coarsening algorithm, with standard strength-of-connection using parameter  $\theta = 0.25$ , classical interpolation, and a V(1,1) cycle with symmetric Gauss-Seidel as the pre- and post-relaxation scheme.

In Figure 6, we compare CGMRES against FGMRES for both the standard and preconditioned linear system, for a fixed number of iterations. In the nonpreconditioned case, both algorithms stagnate in residual. We see that enforcing the dissipation law on CGMRES leads both to an increase in residual norm over the first tens of iterations (in comparison with that of FGMRES), while failing to satisfy the constraints until iteration 12. Here, we note that the SQSLP solver returns not-a-numbers when it fails to converge, leading to our inclusion of the check on Line 18 of Algorithm 2. When this happens, we revert to the regular FGMRES solution computed on Line 14, explaining the concurrence between the residual norms for iterations 3-12. Note also that, for these iterations, the misfit in the mass conservation is larger than the residual norm, showing there is no general relationship between the size of the residual norm and the misfit in the constraints. Even once the Krylov space is rich enough to allow the constraints to be satisfied, we are still far from convergence of the linear system. In contrast, we see similar reduction in residual norm for both CGMRES and FGMRES with the AMG preconditioner. Furthermore, the CGMRES iteration shows immediate satisfaction of the constraints when they are imposed, with no significant deviation in the residual norm until we are well past reasonable stopping tolerances, with the residual norm below  $10^{-9}$ .

FIGURE 6. A comparison between CGMRES as proposed in Section 3.1 and FGMRES for the heat equation. The linear system corresponds to the numerical scheme (2.6) with  $\tau = 0.01$ ,  $M_x = 50$  and degree  $q = 1$ . We initialise  $U^0$  with (4.3) and solve for  $U^1$ , enforcing the constraints (2.2) and using initial guess  $\mathbf{x}_0 = \mathbf{0}$ . Here, we study the effects of preconditioning the linear system using algebraic multigrid (shown at right).



Results in table 2 again show the relative costs of preconditioner setup and solution using classical FGMRES and the CGMRES algorithm proposed here. In particular, we now note that the AMG setup time is on the same order as both solve times (as is typical for AMG), and that the additional cost for the CGMRES

iterations is again primarily due to the overhead of computing the “reduced” constraints over the Krylov space. This cost scales, as expected, with problem size ( $M_x^2$ ) and size of the Krylov space, and is roughly equal to the average cost of a single step of the unconstrained algorithm. Here, we note that the preservation of the constraints is significantly better with CGMRES than with FGMRES, particularly for the mass constraint. When running FGMRES, the constraints generally converge roughly at the same rate as the GMRES residual norm. As seen in Figure 6, this can lead to a large difference in the misfit in the constraints between FGMRES and CGMRES when we converge in 5-6 iterations, as we do here. Thus, while it is true that we could substantially reduce the FGMRES constraint misfit by running one or two more iterations of FGMRES, the cost of doing so would equal or exceed that of the extra overhead for enforcing the constraints once at the end of a CGMRES solve.

TABLE 2. Computational times for a single solve of the heat equation (2.6) preconditioned by Ruge-Stuben AMG for variable spatial mesh resolution,  $M_x$ , with  $\tau = 0.1$ ,  $\epsilon = 10^{-7}$ ,  $\mathcal{E} = 10\epsilon$  and a zero initial guess for  $\mathbf{x}_0$ . We present the preconditioner assembly time (in seconds)  $\mathcal{T}_{\mathcal{P}}$ , total run time of FGMRES (as described in Algorithm 1)  $\mathcal{T}_{\text{gmres}}$ , total run time of CGMRES (as described in Algorithm 2)  $\mathcal{T}_{\text{cgmres}}$ , and total number of iterations for both FGMRES and CGMRES (which are the same in this example). We further break down the costs within CGMRES, writing  $\mathcal{T}_s$  as the average run time for an unconstrained iteration,  $\mathcal{T}_{\text{overhead}}$  as the average computational overhead (per constrained iteration) required to assemble the constraints, and  $\mathcal{T}_c$  as the constrained iteration cost. Here,  $\#(\mathcal{T}_c)$  denotes the number of constrained iterations of CGMRES.

$M_x$	128	256	512	1024	2048
$\mathcal{T}_{\mathcal{P}}$	1.93e-02	5.81e-02	2.35e-01	1.15e+00	4.54e+00
$\mathcal{T}_{\text{gmres}}$	1.69e-02	5.86e-02	2.62e-01	1.19e+00	6.50e+00
$\mathcal{T}_{\text{cgmres}}$	2.28e-02	7.13e-02	3.07e-01	1.41e+00	8.60e+00
Iterations	5	5	5	5	6
$\mathcal{T}_s$	3.72e-03	1.18e-02	5.12e-02	2.30e-01	1.04e+00
$\mathcal{T}_{\text{overhead}}$	3.04e-03	1.03e-02	4.30e-02	2.35e-01	1.05e+00
$\mathcal{T}_c$	4.50e-03	1.28e-02	5.49e-02	2.41e-01	1.12e+00
$\#(\mathcal{T}_c)$	1	1	1	1	2

## 5. CONCLUSION

Here, we introduce a modification to the FGMRES algorithm that allows for conserved quantities of an underlying discretisation to be preserved at any desired stopping tolerance. While we focus on the modification for FGMRES, the approach can be freely applied to any Krylov solver where an explicit basis for the Krylov space is used in a minimisation algorithm. Importantly, the proposed constrained algorithm can be incorporated into existing solver implementations through minor modification, replacing a QR factorisation of the  $(\ell + 1) \times \ell$  Hessenberg matrix with a (nonlinear) constrained optimisation problem in  $\ell + c$  unknowns for  $c$  constraints. We observe (experimentally) that the constrained solver performs no worse than FGMRES, so long as the Krylov space is sufficiently rich and/or the initial guess is sufficiently close to solution. While we focus here on evaluating the method as a proof-of-concept, we believe the experiments are promising enough to justify future work on efficient implementation of this approach in an optimised high-performance computing environment. Such a study could also include the nonlinear variant of this approach, proposed in Remark 3.4.

## REFERENCES

- [1] R. ABU-LABDEH, S. MACLACHLAN, AND P. FARRELL, *Monolithic multigrid for implicit Runge-Kutta discretizations of incompressible fluid flow*, J. Comput. Phys., 478 (2023), p. 111961.

- [2] D. N. ARNOLD, R. S. FALK, AND R. WINTHER, *Finite element exterior calculus, homological techniques, and applications*, Acta Numer., 15 (2006), pp. 1–155, <https://doi.org/10.1017/s0962492906210018>.
- [3] N. BELL, L. N. OLSON, AND J. SCHRODER, *PyAMG: Algebraic multigrid solvers in python*, Journal of Open Source Software, 7 (2022), p. 4142, <https://doi.org/10.21105/joss.04142>.
- [4] P. BENNER AND H. FASSBENDER, *An implicitly restarted symplectic Lanczos method for the Hamiltonian eigenvalue problem*, Linear Algebra Appl., 263 (1997), pp. 75–111, [https://doi.org/10.1016/s0024-3795\(96\)00524-1](https://doi.org/10.1016/s0024-3795(96)00524-1).
- [5] P. BENNER AND H. FASSBENDER, *An implicitly restarted symplectic Lanczos method for the symplectic eigenvalue problem*, SIAM J. Matrix Anal. Appl., 22 (2001), pp. 682–713, <https://doi.org/10.1137/S0895479898343115>.
- [6] P. BENNER, H. FASSBENDER, AND M. STOLL, *A Hamiltonian Krylov–Schur-type method based on the symplectic Lanczos process*, Linear Algebra Appl., 435 (2011), pp. 578–600, <https://doi.org/10.1016/j.laa.2010.04.048>.
- [7] P. BIRKEN AND V. LINDERS, *Conservative iterative methods for implicit discretizations of conservation laws*, arXiv preprint arXiv:2106.10088, (2021).
- [8] S. BLANES AND F. CASAS, *A Concise Introduction to Geometric Numerical Integration*, vol. 23 of Monographs and Research Notes in Mathematics, CRC Press, 2016.
- [9] G. BOGFJELLMO, E. CELLEDONI, R. McLACHLAN, B. OWREN, AND R. QUISPEL, *Using aromas to search for preserved measures and integrals in Kahan’s method*, arXiv preprint arXiv:2209.01094, (2022), <https://doi.org/10.48550/ARXIV.2209.01094>.
- [10] A. BRANDT, S. F. MCCORMICK, AND J. W. RUGE, *Algebraic multigrid (AMG) for sparse matrix equations*, in Sparsity and Its Applications, D. J. Evans, ed., Cambridge University Press, Cambridge, 1984.
- [11] W. L. BRIGGS, V. E. HENSON, AND S. F. MCCORMICK, *A Multigrid Tutorial*, SIAM Books, Philadelphia, 2000. Second edition.
- [12] A. R. CONN, N. I. GOULD, AND P. L. TOINT, *Trust region methods*, SIAM, 2000.
- [13] C. COTTER AND J. THUBURN, *A finite element exterior calculus framework for the rotating shallow-water equations*, J. Comput. Phys., 257 (2014), pp. 1506–1526, <https://doi.org/10.1016/j.jcp.2013.10.008>.
- [14] C. J. COTTER AND J. SHIPTON, *Mixed finite elements for numerical weather prediction*, J. Comput. Phys., 231 (2012), pp. 7076–7091.
- [15] S. C. EISENSTAT AND H. F. WALKER, *Choosing the forcing terms in an inexact Newton method*, SIAM J. Sci. Comput., 17 (1996), pp. 16–32.
- [16] P. E. FARRELL, R. C. KIRBY, AND J. MARCHENA-MENÉNDEZ, *Irksome: Automating Runge–Kutta time-stepping for finite element methods*, ACM Trans. Math. Software, 47 (2021), pp. 1–26, <https://doi.org/10.1145/3466168>.
- [17] A. FROMMER AND U. GLÄSSNER, *Restarted GMRES for shifted linear systems*, SIAM J. Sci. Comput., 19 (1998), pp. 15–26, <https://doi.org/10.1137/s1064827596304563>.
- [18] G. J. GASSNER, *A skew-symmetric discontinuous Galerkin spectral element discretization and its relation to SBP-SAT finite difference methods*, SIAM J. Sci. Comput., 35 (2013), pp. A1233–A1253, <https://doi.org/10.1137/120890144>.
- [19] G. J. GASSNER, A. R. WINTERS, AND D. A. KOPRIVA, *Split form nodal discontinuous Galerkin schemes with summation-by-parts property for the compressible euler equations*, J. Comput. Phys., 327 (2016), pp. 39–66, <https://doi.org/10.1016/j.jcp.2016.09.013>.
- [20] A. GREENBAUM, *Iterative Methods for Solving Linear Systems*, Frontiers in Applied Mathematics, SIAM, Philadelphia, 1997.
- [21] E. HAIRER, C. LUBICH, AND G. WANNER, *Geometric Numerical Integration: Structure-Preserving Algorithms for Ordinary Differential Equations*, vol. 31, Springer, 2nd ed., 2006, <https://doi.org/10.1007/3-540-30666-8>.
- [22] E. HAIRER AND G. WANNER, *Solving ordinary differential equations II*, vol. 375, Springer Berlin Heidelberg, 1996.
- [23] F. H. HARLOW AND J. E. WELCH, *Numerical calculation of time-dependent viscous incompressible flow of fluid with free surface*, Phys. Fluids, 8 (1965), pp. 2182–2189.
- [24] M. HOLEC, B. ZHU, I. JOSEPH, C. J. VOGL, B. S. SOUTHWORTH, A. CAMPOS, A. M. DIMITS, AND W. E. PAZNER, *Arbitrary order energy and enstrophy conserving finite element methods for 2D incompressible fluid dynamics and drift-reduced magnetohydrodynamics*, arXiv preprint arXiv:2202.13022, (2022), <https://doi.org/10.48550/ARXIV.2202.13022>.
- [25] C. HUFFORD AND Y. XING, *Superconvergence of the local discontinuous Galerkin method for the linearized Korteweg-de Vries equation*, J. Comput. Appl. Math., 255 (2014), pp. 441–455, <https://doi.org/10.1016/j.cam.2013.06.004>.
- [26] J. JACKAMAN, *Finite element methods as geometric structure preserving algorithms*, PhD thesis, School of Mathematical, Physical and Computational Sciences, University of Reading, 2018.
- [27] J. JACKAMAN AND S. MACLACHLAN, *Implementation of experiments in ‘Structure Preserving Krylov solvers for structure-preserving discretisations’*, June 2023, <https://doi.org/10.5281/zenodo.7419815>.
- [28] D. KRAFT, *A software package for sequential quadratic programming*, Tech. Report Tech. Rep. DFVLR-FB 88-28, DLR German Aerospace Center – Institute for Flight Mechanics, Köln, Germany, 1988.
- [29] B. LEIMKUHLER AND S. REICH, *Simulating Hamiltonian Dynamics*, vol. 14 of Cambridge Monographs on Applied and Computational Mathematics, Cambridge University Press, 2004, <https://doi.org/10.1017/CBO9780511614118>.
- [30] L. LI AND E. CELLEDONI, *Krylov projection methods for linear Hamiltonian systems*, Numer. Algorithms, 81 (2019), pp. 1361–1378, <https://doi.org/10.1007/s11075-018-00649-8>.
- [31] X. LI, J. DEMMEL, J. GILBERT, I. L. GRIGORI, M. SHAO, AND I. YAMAZAKI, *SuperLU Users’ Guide*, Tech. Report LBNL-44289, Lawrence Berkeley National Laboratory, September 1999. <https://portal.nersc.gov/project/sparse/superlu/ug.pdf> Last update: June 2018.



- [32] X. S. LI AND M. SHAO, *A supernodal approach to incomplete LU factorization with partial pivoting*, ACM Trans. Math. Software, 37 (2010).
- [33] V. LINDERS AND P. BIRKEN, *Locally conservative and flux consistent iterative methods*, arXiv preprint arXiv:2206.10943, (2022), <https://doi.org/10.48550/ARXIV.2206.10943>.
- [34] E. MANSFIELD, G. M. BEFFA, AND J. P. WANG, *Discrete moving frames and discrete integrable systems*, Found Comput Math, 13 (2013), pp. 545–582, <https://doi.org/10.1007/s10208-013-9153-0>.
- [35] J. E. MARSDEN AND M. WEST, *Discrete mechanics and variational integrators*, Acta Numer., 10 (2001), pp. 357–514, <https://doi.org/10.1017/s096249290100006x>.
- [36] F. RATHGEBER, D. A. HAM, L. MITCHELL, M. LANGE, F. LUPORINI, A. T. T. MCRAE, G.-T. BERCEA, G. R. MARKALL, AND P. H. J. KELLY, *Firedrake: automating the finite element method by composing abstractions*, ACM Trans. Math. Software, 43 (2017), pp. Art. 24, 27, <https://doi.org/10.1145/2998441>.
- [37] J. W. RUGE AND K. STÜBEN, *Algebraic multigrid (AMG)*, in Multigrid Methods, S. F. McCormick, ed., vol. 3 of Frontiers in Applied Mathematics, SIAM, Philadelphia, PA, 1987, pp. 73–130.
- [38] Y. SAAD, *Iterative methods for sparse linear systems*, SIAM, Philadelphia, PA, second ed., 2003.
- [39] Y. SAAD AND M. H. SCHULTZ, *GMRES: a generalized minimal residual algorithm for solving nonsymmetric linear systems*, SIAM J. Sci. Statist. Comput., 7 (1986), pp. 856–869, <https://doi.org/10.1137/0907058>.
- [40] J. SANZ-SERNA AND M. CALVO, *Numerical Hamiltonian Problems*, vol. 7 of Applied Mathematics and Mathematical Computation, Chapman & Hall, 1994.
- [41] S. SATO, Y. MIYATAKE, AND J. C. BUTCHER, *High-order linearly implicit schemes conserving quadratic invariants*, arXiv preprint arXiv:2203.00944, (2022), <https://doi.org/10.48550/ARXIV.2203.00944>.
- [42] K. STÜBEN, *An introduction to algebraic multigrid*, in Multigrid, U. Trottenberg, C. Oosterlee, and A. Schüller, eds., Academic Press, London, 2001, pp. 413–528.
- [43] M. TAO, *Explicit symplectic approximation of nonseparable Hamiltonians: Algorithm and long time performance*, Phys. Rev. E, 94 (2016), p. 043303, <https://doi.org/10.1103/physreve.94.043303>.
- [44] U. TROTTEBERG, C. W. OOSTERLEE, AND A. SCHÜLLER, *Multigrid*, Academic Press, London, 2001.
- [45] P. VIRTANEN, R. GOMMERS, T. E. OLIPHANT, M. HABERLAND, T. REDDY, D. COUNAPEAU, E. BUROVSKI, P. PETERSON, W. WECKESSER, J. BRIGHT, S. J. VAN DER WALT, M. BRETT, J. WILSON, K. J. MILLMAN, N. MAYOROV, A. R. J. NELSON, E. JONES, R. KERN, E. LARSON, C. J. CAREY, Í. POLAT, Y. FENG, E. W. MOORE, J. VANDERPLAS, D. LAXALDE, J. PERKTOLD, R. CIMRMAN, I. HENRIKSEN, E. A. QUINTERO, C. R. HARRIS, A. M. ARCHIBALD, A. H. RIBEIRO, F. PEDREGOSA, P. VAN MULBREGT, AND SciPy 1.0 CONTRIBUTORS, *SciPy 1.0: Fundamental Algorithms for Scientific Computing in Python*, Nat. Methods, 17 (2020), pp. 261–272, <https://doi.org/10.1038/s41592-019-0686-2>.
- [46] D. S. WATKINS, *On Hamiltonian and symplectic Lanczos processes*, Linear Algebra Appl., 385 (2004), pp. 23–45, <https://doi.org/10.1016/j.laa.2002.11.001>.
- [47] J. YAN AND C.-W. SHU, *A local discontinuous Galerkin method for KdV type equations*, SIAM J. Numer. Anal., 40 (2002), pp. 769–791, <https://doi.org/10.1137/S0036142901390378>.
- [48] *Software used in ‘Preconditioned Krylov solvers for structure-preserving discretisations’*, dec 2022, <https://doi.org/10.5281/zenodo.7414962>.

JAMES JACKAMAN DEPARTMENT OF MATHEMATICAL SCIENCES, NTNU, 7491 TRONDHEIM, NORWAY [james.jackaman@ntnu.no](mailto:james.jackaman@ntnu.no).

SCOTT MACLACHLAN DEPARTMENT OF MATHEMATICS AND STATISTICS, MEMORIAL UNIVERSITY OF NEWFOUNDLAND, ST. JOHN’S, NL, A1C 5S7, CANADA [smaclachlan@mun.ca](mailto:smaclachlan@mun.ca).